

The First Galaxies

VOLKER BROMM¹ AND NAOKI YOSHIDA²

¹ *Department of Astronomy and Texas Cosmology Center, University of Texas, Austin, Texas 78712; email: vbromm@astro.as.utexas.edu*

² *Institute for the Physics and Mathematics of the Universe, University of Tokyo, Kashiwa, Chiba 277-8583, Japan; email: naoki.yoshida@ipmu.jp*

Key Words cosmology, galaxy formation, intergalactic medium, star formation, Population III

Abstract We review our current understanding of how the first galaxies formed at the end of the cosmic dark ages, a few 100 million years after the Big Bang. Modern large telescopes discovered galaxies at redshifts greater than seven, whereas theoretical studies have just reached the degree of sophistication necessary to make meaningful predictions. A crucial ingredient is the feedback exerted by the first generation of stars, through UV radiation, supernova blast waves, and chemical enrichment. The key goal is to derive the signature of the first galaxies to be observed with upcoming or planned next-generation facilities, such as the *James Webb Space Telescope* or *Atacama Large Millimeter Array*. From the observational side, ongoing deep-field searches for very high-redshift galaxies begin to provide us with empirical constraints on the nature of the first galaxies.

CONTENTS

INTRODUCTION	3
------------------------	---

WHAT IS A FIRST GALAXY?	8
<i>Theoretical Perspective</i>	8
<i>Observational Perspective</i>	11
CONSTRAINTS FROM EXISTING OBSERVATIONS	13
<i>High-redshift Dropout galaxies</i>	14
<i>Lyman-α Emitters</i>	15
THEORETICAL STUDIES	17
<i>Overview</i>	17
<i>Pre-Galactic Metal Enrichment</i>	20
<i>Star Formation in the First Galaxies</i>	22
<i>Radiation from the First Galaxies</i>	25
THE FIRST SUPERMASSIVE BLACK HOLES	29
<i>Formation Models</i>	30
<i>SMBH-First Galaxy Coevolution</i>	33
<i>James Webb Space Telescope SIGNATURE</i>	34
<i>JWST Instruments and Sensitivities</i>	34
<i>Observing High-redshift Sources</i>	36
<i>Modelling Star Formation in the First Galaxies</i>	38
<i>Source Number Counts</i>	40
STELLAR ARCHAEOLOGY	42
<i>Ultrafaint Dwarf Galaxies</i>	43
<i>Theoretical Models</i>	44
OUTLOOK	47

1 INTRODUCTION

The first galaxies have captivated theorists and observers alike for more than four decades. They were recognized as key drivers of early cosmic evolution at the end of the cosmic dark ages, when the Universe was just a few 100 million years old (e.g., Rees 1993; Barkana & Loeb 2001). Within the standard Λ cold dark matter (Λ CDM) cosmology, where structure forms hierarchically through mergers of smaller dark matter (DM) halos into increasingly larger ones, the first galaxies were the basic building blocks for galaxy formation (e.g., Blumenthal et al. 1984; Springel et al. 2005). The highly complex physics associated with galaxy assembly and evolution still largely defies our understanding, but the first galaxies may provide us with an ideal, simplified laboratory for study (e.g., Loeb 2010).

A crucial ingredient to any theory of how the first galaxies assembled, and how they impacted subsequent cosmic history, is the feedback exerted by the stars formed inside them or their smaller progenitor systems (e.g., Wise & Abel 2008; Greif et al. 2010). Understanding the first galaxies is therefore intricately linked to the formation of the first, so-called Population III (Pop III) stars (Bromm et al. 2009). The stellar feedback is usually divided into radiative and supernova (SN) feedback (Ciardi & Ferrara 2005). The radiative effect consists of the build-up of HII regions around individual massive Pop III stars, thus initiating the extended process of cosmic reionization (Sokasian et al. 2004; Barkana & Loeb 2007). The SN feedback has a direct mechanical aspect, where the blastwave triggered by the explosion imparts heat and momentum to the surrounding intergalactic medium (IGM). Supernovae also disperse heavy elements into the IGM, thereby affecting the subsequent mode of star formation in the polluted gas. An early

episode of enriching the primordial, pure H/He Universe with metals is therefore another long-term legacy left behind by the first stars and galaxies, together with reionization.

There is a further, observational, reason for the current flurry of activity in understanding the first galaxies. Researchers wish to predict the properties of the sources to be probed with upcoming or planned next-generation facilities, such as the *James Webb Space Telescope (JWST)*, the *Atacama Large Millimeter Array (ALMA)*, or extremely large telescopes to be constructed on the ground. The main efforts in the latter category are the *Giant Magellan Telescope*, the *Thirty Meter Telescope*, and the *European Extremely Large Telescope*, which are pursued concurrently at the present time. In each case, we need to work out the overall luminosities, spectral energy distributions or colors, and the expected number densities of sources as a function of redshift. Complementary to the direct detection approach are possible signatures of the first galaxies in the redshifted 21-cm background radiation (Furlanetto et al. 2006; Morales & Wyithe 2010). Here, a number of already operational or planned meter-wavelength radio telescopes, among them the Low Frequency Array (LOFAR), will soon commence the search for the 21-cm signatures. The effort of arriving at robust predictions for these facilities greatly benefits from recent advances in supercomputer technology, where large- (tera and peta-) scale, massively parallel systems provide us with unprecedented computational power to carry out ever more realistic simulations in the cosmological context.

Most large galaxies today harbor supermassive black holes (SMBHs) in their centers (e.g., Kormendy & Richstone 1995; Ferrarese & Ford 2005). An important question then is when and how galaxies first acquired such central black holes.

Related is the problem of understanding the presence of $\sim 10^9 M_\odot$ SMBHs that are inferred to power the luminous quasars discovered by the Sloan Digital Sky Survey (SDSS) at redshifts $z \gtrsim 6$ (Fan, Carilli & Keating 2006). A popular theoretical model assumes that such very massive black holes grew from smaller seeds, present already in the smaller progenitor systems that merged into the massive SDSS quasar hosts (Li et al. 2007). The efficiency of growing a black hole via accretion of surrounding gas over the available time of several hundred million years, however, may have been quite limited. A possible way out is to begin the SMBH assembly process already with more massive seeds. The first galaxies have indeed been suggested as viable formation sites for such $\sim 10^6 M_\odot$ seed black holes (see Section 5). Regardless of their exact properties and origin, such massive black holes would likely have influenced the structure and evolution of the first galaxies (e.g., Cattaneo et al. 2009).

The nature of the stellar populations in the first galaxies is crucial for the observational quest. According to some theories, the majority of the first galaxies already contained low-mass, Population II (Pop II), stars, and perhaps stellar clusters in general. This expectation is based on the theory of a ‘critical metallicity’, $Z_{\text{crit}} \sim 10^{-6} - 10^{-4} Z_\odot$, above which the mode of star formation is thought to change from top-heavy to normal, bottom-heavy (e.g., Bromm et al. 2001; Schneider et al. 2002). Due to the pre-enrichment from Pop III stars in the galaxy’s progenitor systems, the so-called minihalos (Haiman, Thoul & Loeb 1996; Tegmark et al. 1997; Yoshida et al. 2003), the first galaxies were likely already supercritical, thus experiencing Pop II star formation. The minihalos, consisting of DM halos with total mass $\sim 10^6 M_\odot$ and collapsing at $z \sim 20 - 30$, are the formation sites for the first (Pop III) stars. Cooling inside of them relies

on a trace amount ($\sim 10^{-3}$ by number) of molecular hydrogen. These halos have shallow potential wells, so that they are highly susceptible to negative feedback effects from Pop III stars. A subset of the first Pop II star, those with subsolar masses, will survive to the present, and can thus be probed as fossils of the dark ages in our immediate cosmic neighborhood. This approach, often termed stellar archaeology (e.g., Beers & Christlieb 2005; Frebel 2010), provides constraints on the SN yields of the first stars, as well as on the environment for star formation inside the first galaxies. A similar strategy has recently become feasible, where the stellar content and structural properties of low-mass dwarf galaxies in the Local Group are interpreted under the assumption that they are descendants of the first galaxies (e.g., Tolstoy, Hill & Tosi 2009; Ricotti 2010). Finally, these early galaxies are also discussed as formation sites for the oldest globular clusters (Bromm & Clarke 2002; Kravtsov & Gnedin 2005; Moore et al. 2006; Brodie & Strader 2006; Boley et al. 2009; Cooper et al. 2010).

The plan for this review is as follows. We begin by considering the seemingly straightforward question: What is the definition of a first galaxy? It turns out that there is no universally accepted definition, as is the case for what we mean by the formation of the first stars. Theorists and observers employ different concepts, and often do not agree even among themselves. We will try to clarify the situation (Section 2). We then turn to a survey of what is known from existing observations that push the envelope and begin to reach very high redshifts (Section 3). This is followed by a more extended discussion of the lessons gleaned from recent simulations, many of them studying the assembly of the first galaxies with considerable physical sophistication and within a realistic cosmological context (Section 4). Due to its importance, we devote a separate section to the early

co-evolution of massive black holes and stellar systems, although our knowledge here also relies mostly on theory and numerical simulations (Section 5). The following two sections discuss the observational signature of the first galaxies, with a special focus on the *JWST*, but also addressing the stellar archaeology approach, as well as more indirect clues from the cumulative impact of the first galaxies on reionization, 21cm radiation, and the cosmic infrared background (Sections 6 – 7). We conclude with a brief outlook into the exciting decade ahead.

At the end of this introduction, we would like to point the reader to a few other reviews that cover material related to this subject here. For a general overview of the end of the cosmic dark ages, see the extensive review by Barkana & Loeb (2001), the more succinct one by Bromm et al. (2009), and the monographs by Stiavelli (2009) and Loeb (2010). Feedback processes are discussed in detail by Ciardi & Ferrara (2005), whereas the physics and observational picture of reionization are treated by Fan et al. (2006), Barkana & Loeb (2007), and Meiksin (2009). The formation of the first stars was reviewed by Bromm & Larson (2004) and Glover (2005). It is instructive to consider the huge lore of knowledge that we have on present-day star formation, when extrapolating to the primordial case. Comprehensive resources are the reviews by McKee & Ostriker (2007) and Zinnecker & Yorke (2007). The field of stellar archaeology has been summarized by Freeman & Bland-Hawthorn (2002), Beers & Christlieb (2005), Tolstoy, Hill & Tosi (2009), Frebel (2010), and Ricotti (2010). Finally, Mo, van den Bosch & White (2010) have written an excellent textbook that summarizes all aspects of galaxy formation and evolution in the proper cosmological context (also see Benson 2010).

2 WHAT IS A FIRST GALAXY?

There is currently no universally agreed upon definition of what we mean by “first galaxy”. Observers and theorists operate with different working hypotheses, and those hypotheses have changed with our evolving understanding. We here summarize the most common attempts to define a primordial galaxy. Intriguingly, to properly pose the question (“What is a first galaxy?”), we already need to know the answer to it. It is thus likely, that we will witness a continuing iterative process, but it is also evident that devising a proper definition must be part of the discovery process.

2.1 Theoretical Perspective

On the theory side, the discussion typically begins with an enumeration of defining properties. What are the ingredients required for a first galaxy ? For a galaxy in general, the presence of a confining dark matter halo hosting a long-lived stellar system seems inevitable. Often, there is gas present as well, but there are galaxies without any apparent gas. In addition, we may stipulate that the potential well of the DM halo is sufficiently deep to retain gas that was heated to temperatures in excess of $\sim 10^4$ K as a result of photo-ionization by stellar radiation (Mesinger & Dijkstra 2008; Mesinger, Bryan & Haiman 2009). More stringently, we may also want to demand that the halo can retain gas heated and accelerated through SN explosions. Finally, we may ask whether the system is able to support a multi-phase interstellar medium, which in turn could sustain a stable mode of self-regulated star formation.

The theorists’ debate now centers on identifying the smallest, lowest-mass, DM halos that fulfill the criteria listed above. According to the tentative list of

criteria for what constitutes a galaxy, DM halos that are unable to form stars and therefore remain dark would not be galaxies. This would in particular apply to the first DM halos to collapse, or virialize, at $z \sim 100$. Their mass scale strongly depends on the nature of the CDM particle (Diemand, Moore & Stadel 2005). For DM consisting of weakly interacting massive particles, as predicted by the theory of supersymmetry, the first DM halos comprise a mass of $\sim 10^{-6} M_{\odot}$, roughly the mass of Earth. For axion DM, on the other hand, the smallest halos would only contain $\sim 10^{-13} M_{\odot}$. Returning to the discussion of those DM halos that are able to form stars, one class of models proposes minihalos, defined in Section 1, as hosts for the first galaxies (Ricotti, Gnedin, & Shull 2002a, 2002b, 2008). In this case, the halos that host the formation of the first (Pop III) stars would coincide with the first galaxies. This *Ansatz*, however, makes the implicit assumption that the initial mass function (IMF) of the first stars was not very different from the locally observed one, where the distribution peaks at low masses around $< 1 M_{\odot}$. Negative feedback effects from them, in terms of star-formation efficiency, would not be so severe for a subset of minihalos, such that they could sustain star formation and effectively self-enrich.

Assuming that primordial stars were predominantly massive, as is suggested by most current theoretical models and simulations (Omukai & Palla 2003; Bromm et al. 2009), leads to a very different picture, though. After the first stars are formed inside a minihalo, vigorous negative feedback effects would effectively shut off the potential for subsequent star formation. For once, the heating due to photo-ionization drives a pressure wave that greatly suppresses the gas density inside of minihalos (Kitayama et al. 2004; Whalen, Abel & Norman 2004; Alvarez, Bromm & Shapiro 2006). If, in addition, energetic SNe occurred, the

minihalo would be virtually devoid of any gas, leaving behind a sterile system as far as star formation is concerned (Bromm, Yoshida & Hernquist 2003; Greif et al. 2007). More massive systems that are able to re-assemble the high-entropy material affected by Pop III stars inside minihalos might therefore be needed. There are, however, studies of the SN feedback in primordial minihalos that suggest a different conclusion (Whalen et al. 2008). If the bulk of the minihalo were to remain substantially neutral, thus not triggering such dramatic outflows and the corresponding density suppression, the SN remnant would be highly radiative and largely confined to the minihalo, thus effectively self-enriching them. The condition of near-neutrality would be satisfied in more massive ($\sim 10^7 M_\odot$) minihalos (Kitayama & Yoshida 2005), combined with not too massive Pop III progenitor stars. It is an open question whether these conditions are ever met in a realistic cosmological setting, where Pop III star formation first occurred in lower-mass systems.

To gauge how susceptible a given halo will be to negative stellar feedback, it is useful to introduce its virial temperature

$$T_{\text{vir}} = \frac{\mu m_{\text{H}} V_c^2}{2k_{\text{B}}} \simeq 10^4 \left(\frac{\mu}{0.6} \right) \left(\frac{M}{10^8 M_\odot} \right)^{2/3} \left[\frac{\Delta_c}{18\pi^2} \right]^{1/3} \left(\frac{1+z}{10} \right) \text{ K}, \quad (1)$$

where V_c is the circular velocity, μ is the mean molecular weight, and Δ_c gives the density contrast established through virialization as a function of redshift (Bryan & Norman 1998). Closely related is the gravitational binding energy of the halo

$$E_b = \frac{1}{2} \frac{GM^2}{r_{\text{vir}}} \simeq 5 \times 10^{53} \left(\frac{M}{10^8 M_\odot} \right)^{5/3} \left[\frac{\Delta_c}{18\pi^2} \right]^{1/3} \left(\frac{1+z}{10} \right) \text{ erg}, \quad (2)$$

where r_{vir} is the virial radius of the halo. In evaluating these expressions, we have assumed cosmological parameters as recently determined by the *Wilkinson*

Microwave Anisotropy Probe (WMAP) (Komatsu et al. 2009), and that $z \gg 1$.

Another series of recent simulations has suggested that DM halos containing a mass of $\sim 10^8 M_\odot$ and collapsing at $z \sim 10$ were the hosts for the first *bona fide* galaxies (Wise & Abel 2007, 2008; Greif et al. 2008, 2010). These dwarf systems can indeed re-virialize the gas that was affected by previous star formation in minihalos (see **Figure 1**). They are special in that their associated virial temperature exceeds the threshold, $\sim 10^4$ K, for cooling due to atomic hydrogen (Oh & Haiman 2002). These so-called ‘atomic-cooling halos’ did not rely on the presence of molecular hydrogen to enable cooling of the primordial gas. In addition, their potential wells were sufficiently deep to retain photoheated gas, in contrast to the shallow potential wells of minihalos (Dijkstra et al. 2004). Our tentative conclusion is that atomic cooling halos thus seem to fulfill the requirements for a first galaxy, but important open questions remain that need to be addressed with future simulations (see Section 4).

A related issue is to identify the conditions that enable the formation of the first disk galaxies (Pawlik, Milosavljevic & Bromm 2011), or of central supermassive black holes (see Section 5). However, such disks and central black holes may well have emerged only at a later stage of hierarchical structure formation, *after* the first galaxies had already formed. In this regard, they would not be necessary ingredients for a first galaxy, although they may well have been prevalent at the highest redshifts.

2.2 Observational Perspective

From the observational side, there are two main operational definitions employed.

One may simply equate “first galaxy” with the highest redshift galaxies observ-

able at a time, given its technology is pushed to the very limit. Currently, with a combination of *Hubble Space Telescope* (HST) photometry and ground-based 8-10m class spectroscopy, this allows us to see galaxies at $z > 7$, with a record of $z \simeq 8.6$ (Iye et al. 2006; Bouwens et al. 2010a; Lehnert et al. 2010), or possibly even of $z \sim 10$ (Bouwens et al. 2011). Evidently, this is a moving target, and such a temporary definition makes it hard to provide a focus for theoretical studies. In general, a number of galaxies at different evolutionary stages will be present concurrently at a given redshift. Thus it would clearly be preferable if a definition involved some unambiguous criteria, based on the underlying physics.

A more precise definition is to search for galaxies with zero metallicity, or one that hosts predominantly Pop III stars. This popular definition of a first galaxy may however be misleading, and may render any attempts to find first galaxies futile from the very outset. This is because most first galaxies could be already metal-enriched by SNe triggered by the first stars. Recent simulations have indicated that heavy element production and dispersal was very rapid, leading to a bedrock of pre-galactic enrichment after only a few Pop III stars had formed (see Section 4). Indeed, some models predict that the first galaxies predominantly already hosted Pop II stars (Greif et al. 2010; Maio et al. 2011). In summary, we will employ the following tentative definition of “first galaxy” in this review: a galaxy comprised of the very first system of stars to be gravitationally bound in a dark matter halo, regardless of whether the stars are Pop III or Pop II.

In concluding this section, we would like to briefly comment on the concept of a “protogalaxy”, which is now largely only of historical interest. The idea was that a mature galaxy like our Milky Way (MW) more or less evolved in a monolithic fashion (Eggen, Lynden-Bell & Sandage 1962; hereafter ELS), and

not in the hierarchical, bottom-up way that is now widely favored within the standard Λ CDM model. One could then go back in time, making predictions for the luminosity and color of such systems during their initial, monolithic, collapse at high z (Partridge & Peebles 1967). First galaxy then referred to this initial collapse phase. In many ways, defining, and understanding, the first galaxies in a hierarchical context is more difficult than it would have been in a simple ELS model of galaxy formation.

3 CONSTRAINTS FROM EXISTING OBSERVATIONS

An array of observations are now available that provide information, either direct or indirect, on galaxy formation and structure formation in the early Universe. Indirect observations include the large angular-scale polarization in the cosmic microwave background (CMB), recently measured by *WMAP*, as well as the amplitude and fluctuations of the cosmic near-infrared background (CIB). We will discuss these later, and focus here on the search for discrete sources at the highest redshifts.

Available large telescopes, in space and on the ground, are capable of taking images of distant galaxies and/or obtaining spectroscopic data, reaching all the way to the currently highest-redshift galaxy at $z = 8.6$ (Lehnert et al. 2010). There are two main techniques to locate $z > 6$ galaxies, both based on the spectral imprint of hydrogen. In the first case, broad-band photometry aims at identifying absorption breaks due to neutral hydrogen in the vicinity of the source, and in the second case, narrow-band techniques target the strong emission in the Lyman- α line (Stiavelli 2009).

3.1 High-redshift Dropout galaxies

Utilizing the exquisite near-IR sensitivity of the newly installed Wide Field Camera 3 (WFC3) on board the HST, deep images of the Hubble Ultra Deep Field (HUDF) and other fields opened up an unprecedented window into the distant Universe (see **Figure 2**). High-redshift galaxies were identified by the so-called dropout technique, using multi-band imaging (for a recent review, see Robertson et al. 2010).

The galaxy luminosity function (LF) at $z \sim 7$ was derived from the combined observations by HST and large ground-based telescopes (Bouwens et al. 2010c; Ouchi et al. 2009; Castellano et al. 2010). Wide-field observations using the ground-based telescopes are important to determine the bright-end of the LF, whereas HST is able to detect fainter galaxies. The LF is fit by a Schechter function which is described by a power-law towards the faint end such that $\propto L^{-\alpha}$ (see **Figure 3**). The faint-end slope is a critical quantity to derive the global star formation rate density and to estimate the ionizing photon budget for hydrogen reionization (Stiavelli, Fall & Panagia 2004). Although the current data generally suggests a steep power-law with $\alpha \sim 1.7 - 1.9$, it does not yet allow researchers to make a precise determination of α . More data to be acquired by the Cosmic Assembly Near-Infrared Deep Extragalactic Legacy Survey¹ (CANDELS) using HST will reduce the uncertainty in the faint-end slope substantially.

The newly-discovered galaxies beyond $z \sim 7$ appear to be quite “blue”. It is convenient to characterize a galaxy’s stellar population by the UV spectral slope, β , where the flux density is: $f_\lambda \propto \lambda^\beta$. The $z \sim 7$ galaxies show an unusually hard UV continuum with $\beta < -3$, with fainter sources having bluer continuum

¹<http://candels.ucolick.org/>

(Bouwens et al. 2010b,c; Finkelstein et al. 2010). This is in pronounced contrast with local starburst galaxies and Lyman-break galaxies at $z < 6$ that have typically $\beta \sim -2$. Interestingly, the steep continua of the $z \sim 7$ galaxies can be accounted for by stars with very low metallicities, $Z < 5 \times 10^{-4} Z_{\odot}$ (Taniguchi, Shioya & Trump 2010).

The star formation history of individual galaxies can be inferred from the mass density of long-lived stars. Infrared observations by the *Spitzer Space Telescope* provided information on the color, or shape of the spectral energy distribution (SED), of high- z galaxies. The data have been used to estimate the stellar mass and approximate star formation histories of those galaxies (Eyles et al. 2007; Stark et al. 2007; Labbe et al. 2010). Luminous $z \sim 7$ galaxies have stellar masses of 10^9 – 10^{10} solar masses (see **Figure 4**). Obviously these luminous galaxies are not the first galaxies of our definition, but likely are *descendants* of the first galaxies. A sample of $z \sim 7$ galaxies shows evidence of extended star formation over a mean period of 300 Myr (Gonzalez et al. 2010). This is indicative that star formation in these galaxies and their progenitors must have begun at redshifts $z > 10$ (Mobasher et al. 2005; Wiklind et al. 2008). The $z \sim 7$ galaxies may thus have preserved the signature of star and galaxy formation in the pre-reionization era.

3.2 Lyman- α Emitters

There is another population of high-redshift galaxies, characterized by strong Lyman- α line emission. The LF of the Lyman- α emitters (LAEs) has been obtained by Hu et al. (2004) and by Malhotra & Rhoads (2004), and more recently by observations with the Subaru telescope (Ouchi et al. 2010; Hu et al. 2010).

The evolution of the LAE LF across a redshift of six is particularly interesting because the observed Lyman- α luminosity of a galaxy can be significantly affected by neutral hydrogen in the IGM (see **Figure 5**). The evolution of the IGM density and the neutral fraction can be imprinted in the apparent LF of LAEs (Dijkstra, Wyithe & Haiman 2007; Iliev et al. 2008; Dayal, Ferrara & Gallerani 2008). Even the local and large-scale velocity field of the IGM affect the line profile and luminosity of individual galaxies (Dijkstra & Wyithe 2010; Zheng et al. 2010). Recent observations by Kashikawa et al. (2006), Ouchi et al. (2009) and Hu et al. (2010) showed that the LF evolution from $z=5.7$ to $z=7$ is small. The abundance of LAEs decreases at $z > 5.7$, indicating either that there was a slight change in the neutral fraction of the IGM over the time, or that the galaxies themselves evolved. Because of radiative transfer effects for Lyman- α photons with their large absorption and scattering cross-sections, the relationship between the intrinsic Lyman- α luminosity and the apparent, i.e., observed, one is rather involved. The appearance of LAEs depends on density and velocity structures of the IGM surrounding them (McQuinn et al. 2007; Zheng et al. 2010). LAEs themselves could be sources of reionization, which decrease the neutral fraction of the IGM in their vicinities. Interpreting the LF function evolution is thus difficult. Large-volume cosmological simulations with Lyman- α radiative transfer will be needed to quantify and more fully understand this complex interplay.

An important question is what the dominant sources of reionization are. The available observations robustly show that the currently probed high-redshift galaxies, presumably the most luminous ones at the respective epochs, are not the dominant sources of reionization. This is evident by simply counting the total number of ionizing photons from the observed galaxies, and comparing them with

the critical ionizing photon production rate for reionization (Madau, Haardt & Rees 1999; Robertson et al. 2010). There must have been many more faint galaxies that contributed as reionization sources. Interestingly, even if one integrates the currently estimated LF to the very faint end, the estimated ionizing photon budget still falls short of what is required to reionize the Universe (Ouchi et al. 2009). Apparently, faint galaxies must have had large photon escape fractions, and/or harbored stars with a more top-heavy IMF. Alternatively, there may have been different types of early sources of reionization, such as mini-quasars and massive Pop III stars (Ricotti & Ostriker 2004; Sokasian et al. 2004; Kuhlen & Madau 2005).

4 THEORETICAL STUDIES

4.1 Overview

The formation of the first galaxies is an intrinsically more complex process, compared to the appealing simplicity of how the first stars formed. In the latter case, the initial conditions are cosmologically determined, and the relevant physical processes are virtually all known (e.g., Yoshida, Omukai & Hernquist 2008). In the standard hierarchical (Λ CDM) structure formation model, the first generation of stars is formed before galaxies emerged. Feedback effects from these stars are thus expected to play a key role in setting the scene, *i.e.*, *the initial conditions*, for first galaxy formation (see **Figure 1**). In turn, the nature of the first stars may be imprinted in various properties of the first galaxies.

4.1.1 FORMATION EPOCH When did the first galaxies form? This is an intricate question, because it is directly related to the definition of ‘first galaxy’, as discussed in Section 2. If minihalos were the hosts of the first galaxies (Ricotti,

Gnedin, & Shull 2002a, 2002b, 2008), the very first galaxies would be formed at $z > 40$ within standard Λ CDM cosmology (Miralda-Escudé 2003; Naoz, Noter & Barkana 2006). However, it is more plausible that continuous star-formation can be sustained in larger mass dark matter halos, where at least atomic hydrogen cooling operates efficiently. Such large halos with virial temperatures greater than $\sim 10^4$ K are significantly biased objects at $z > 15$ (Miralda-Escudé 2003; Gao et al. 2007). The abundance of the rare density peaks sensitively depends on the assumed cosmological parameters, most notably on the fluctuation amplitude of the initial density field at the relevant mass (length) scales. Typically, such atomic cooling halos, corresponding to $\sim 2\sigma$ -peaks in the Gaussian random field of initial density perturbations, are predicted to form at $z \sim 10 - 15$, or roughly 500 Myr after the Big Bang. Thus, the epoch of the first galaxies lies just beyond the current horizon of observability, and the *JWST* or the next-generation, 30-40m, ground-based telescopes will be able to detect them.

4.1.2 STELLAR FEEDBACK A key element in the physics of first galaxy formation is the feedback from the first stars, and the complications arising from it. If the first stars were massive, they would have exerted a strong influence on the gas in the host halo by injecting significant energy either by radiation or by supernova explosions. Then the next episode of star formation was likely to be delayed for a long time, comparable to the dynamical time of the massive halo, even if the halo's virial temperature well exceeds 10^{4-5} K. Specifically, delay times of a few 10^7 yr are predicted, which corresponds to a significant fraction of the Hubble time at $z \sim 15$. Cosmological simulations performed so far generally support the notion (Johnson & Bromm 2007; Yoshida et al. 2007a; Alvarez, Wise & Abel 2009). The strength of the feedback effect could in principle be reflected

in the very faint-end shape of the luminosity function of high-redshift ($z > 7$) galaxies (Haiman 2009). The characteristic mass of the first stars, ultimately driving the strength of the negative feedback, may thus be constrained.

4.1.3 CONDITIONS FOR STAR FORMATION When we approach the assembly of the first galaxies, the degree of complexity is greatly enhanced compared to the simplicity that governed the formation of the very first stars. In particular, this emerging complexity set the stage for the second generation of star formation that occurred inside the first galaxies. The existence of heavy elements, and possibly of dust grains, the degree of turbulence, and the likely presence of dynamically significant magnetic fields all need to be taken into account. External radiation fields, either from nearby stars and galaxies, or built up globally, also regulated the formation of molecular gas clouds (Ahn & Shapiro 2007; Johnson, Greif & Bromm 2007; Susa 2008). Star formation in the first galaxies is thus as complicated as present-day star formation, and may also be qualitatively similar. Recent cosmological hydrodynamical simulations confirmed that strong turbulence develops within large, proto-galactic halos (Wise & Abel 2007; Greif et al. 2008). Turbulence is generated by supernova explosions or dynamically through dark matter halo mergers, or more generally as a result of gravity-driven virialization. The turbulence is typically supersonic, related to the cold-flow accretion streams that feed gas into the very centers of the first galaxies (see **Figure 6**). In the presence of rapid cooling by atomic hydrogen and by heavier atoms such as carbon, oxygen and iron, the turbulent gas might settle into rotationally supported, central disks (Wise & Abel 2007). We thus have obtained a much improved picture of the physical conditions just prior to the onset of the initial starburst inside the first galaxies.

4.1.4 SIMULATED VERSUS OBSERVED GALAXIES Current state-of-the-art cosmological simulations followed the formation of objects with still rather low masses, typically $\sim 10^8 M_\odot$. The real target of the next-generation telescopes, however, will be those with masses $\gtrsim 10^9 M_\odot$ (Mashchenko, Wadsley & Couchman 2008; Pawlik, Milosavljevic & Bromm 2011). Therefore, there still remains a large gap between the available highly-resolved, ab initio simulations and the realistic targets for the upcoming observations. For the simulation community, much work is still required in building the bridge to the observations. We already know the rough outlines of the $\gtrsim 10^9 M_\odot$ halo formation problem though. Semi-analytic models of galaxy formation combined with large-volume cosmological simulations show that such “luminous” galaxies appear as early as $z \sim 15 - 20$ (Springel et al. 2005; Lacey et al. 2010). A concerted use of both of these approaches, semi-analytical and ab-initio simulations, will be needed to address the many important questions about the formation of the first galaxies (Benson 2010; Raicevic, Theuns & Lacey 2011).

4.2 Pre-Galactic Metal Enrichment

The first galaxies are plausible sources of heavy elements that existed in the IGM at high redshifts (Songaila et al. 2001; Simcoe 2006; Ryan-Weber et al. 2009). The IGM metallicity evolution can place constraints on the prior star formation history (Maio et al. 2011). Although it has also been proposed that Pop III stars, formed in minihalos, can contribute to early chemical evolution (Yoshida et al. 2004; Tornatore, Ferrara & Schneider 2007; Greif et al. 2007), recent observations suggest that the CIV abundance declines at $z > 6$ (Becker, Rauch & Sargent 2009). It is therefore likely that the heavy elements were dispersed

by galaxies that had formed around $z \sim 6$. Assuming that the first galaxies are the dominant source of the IGM enrichment *and* reionization, one should be able to build a consistent model for the reionization history, the galaxy luminosity function and its evolution, as well as the stellar population and chemical evolution in the first galaxies (Choudhury & Ferrara 2006).

Galactic scale outflows driven by radiation pressure from hot stars and/or by supernovae can transport heavy elements into the IGM (Madau, Ferrara & Rees 2001; Mori, Ferrara & Madau 2002; Wada & Venkatesan 2003). How exactly this happened during the reionization epoch can be inferred by comparing the metallicity evolution and the star-formation history. The currently available data seem to point to delayed enrichment via galactic outflows, rather than prompt enrichment (Kramer, Haiman & Madau 2010). Three-dimensional cosmological simulations consistently show that the IGM metal pollution is patchy, leaving a large volume of unpolluted, chemically pristine regions at $z > 6$ (Bertone, Stoehr & White 2005; Tornatore, Ferrara & Schneider 2007). One possible implication of such inhomogeneous enrichment is the existence of Pop III star clusters or SN explosions at lower redshifts, $z < 6$ (Scannapieco et al. 2005; Johnson 2010). Such objects, if they existed, would be an exciting target for direct observations with the *JWST* and future 30-40m ground-based telescopes.

Inside individual first galaxies, the mixing of heavy elements can occur rapidly. Hydrodynamic simulations confirmed this, showing that a large volume of the halo gas in the first galaxies is already metal-enriched before it condenses again to trigger the next episode of star formation (Greif et al. 2010; JH Wise et al., submitted). Specifically, metallicities inside the first galaxies prior the the initial starburst can reach average levels of already $\sim 10^{-3}Z_{\odot}$, with maximum

levels even up to an order of magnitude higher (see **Figure 7**). The degree of mixing and details of the chemical enrichment history can be studied by the very promising approach of stellar archaeology (Section 7). In particular, the metallicity distribution and the relative elemental abundance patterns of stars in dwarf galaxies in the Local Group may preserve the fossil record of early chemical enrichment.

4.3 Star Formation in the First Galaxies

Outstanding questions regarding star-formation in the first galaxies are the star-formation efficiency, the stellar IMF, and the strength of stellar feedback. These three elements are indeed closely connected to each other. The star-formation efficiency is largely affected by the ability of the halo gas to cool and condense. Because the gas density is low initially, cooling by atomic heavy elements such as carbon, oxygen, and iron is effective in early phases (Bromm et al. 2001; Bromm & Loeb 2003a; Santoro & Shull 2006; Omukai et al. 2005; Maio et al. 2010). Unlike hydrogen molecules, which are fragile to soft UV radiation in the Lyman-Werner (LW) bands, cooling by metallic atoms and ions can operate even under the influence of a UV radiation field (Maio et al. 2007; Safranek-Shrader, Bromm & Milosavljevic 2010).

The stellar IMF is more difficult to address. Observationally, at least for local star-forming regions, it is well determined to peak at roughly solar masses and to exhibit a power-law extension towards higher masses: $dN/d\ln M \propto M^x$ with $x \sim -1.35$ (Salpeter 1955; Zinnecker & Yorke 2007). However the mechanism that shapes the IMF is not well understood even in the local Universe. It is often thought that predicting the IMF for the first stars would be simpler in many ways,

and that it would be more top-heavy, with stars more massive than a few tens of solar masses being predominant (for a review of the argument, see Bromm & Larson 2004). In the first galaxies, there are a number of physical ingredients that have been suggested to significantly affect the IMF: supersonic turbulence (Wise & Abel 2008; Greif et al. 2008; 2010), atomic cooling by heavy elements (Bromm et al. 2001; Santoro & Shull 2006; Smith, Sigurdsson & Abel 2008), cooling by dust (Schneider et al. 2006; Omukai et al. 2005), the angular momentum transfer and heating due to magnetic fields (Schleicher et al. 2010), the initial degree of ionization (Nagakura & Omukai 2005; Johnson & Bromm 2006; Yoshida, Omukai & Hernquist 2007; Cazaux & Spaans 2009), and a lower floor to the attainable gas temperature set by the CMB (Larson 1998; Schneider & Omukai 2010). All these processes acted to render star formation in the first galaxies similar again to the present-day case. In particular, the presence of supersonic turbulence likely allowed the formation of multiple stars in a molecular cloud, with a broad mass spectrum that may have resembled the local self-similar form towards high masses. This expectation, however, still needs to be tested with sophisticated simulations.

The ionization degree is important particularly for a primordial gas. The IGM can be ionized by radiation from the first stars (Kitayama et al. 2004; Whalen et al. 2004), blastwaves driven by the first supernovae (Bromm et al. 2003; Machida et al. 2005), by cosmic rays (Vasiliev & Shchekinov 2006; Jasche, Ciardi & Ensslin 2007; Stacy & Bromm 2007), by X-rays emitted from early mini-quasars (Oh 2001; Ricotti & Ostriker 2004; Kuhlen & Madau 2005), or through dark matter annihilation/decay (Ripamonti, Mappeli & Ferrara 2007; Iocco et al. 2008; Spolyar, Freese & Gondolo 2008). An initially ionized gas of primordial

composition can cool to ~ 100 K, where cooling by hydrogen deuteride (HD) molecules becomes important. The abundance of additional free electrons here catalyzes a boost in H_2 formation, which in turn leads to the build-up of a critical abundance of HD, thus enabling this low-temperature cooling channel (e.g., Johnson & Bromm 2006). Primordial stars formed under this condition, the so-called Population III.2 stars (McKee & Tan 2008; Bromm et al. 2009), are thought to include ordinary massive stars (Johnson & Bromm 2006; Yoshida, Omukai & Hernquist 2007; Clark et al. 2011). However the relative importance of Pop III.2 stars remains uncertain (Trenti & Stiavelli 2009; Wolcott-Green & Haiman 2010). If Pop III.1 and Pop III.2 stars have different characteristic masses, detection of high-redshift supernovae of different types, pair-instability SNe and core collapse SNe, will provide constraints on the relative formation rates of PopIII.1 and PopIII.2 stars.

Because of the chemical feedback discussed in Section 4.2, many stars in the first galaxies are probably metal enriched. Detailed calculations on the thermal evolution of a low-metallicity gas have been carried out (Schneider et al. 2002; Jappsen et al. 2007; Omukai, Hosokawa & Yoshida 2010). The results suggest that dust thermal emission remains an efficient cooling mechanism up to very high densities where atomic line cooling is ineffective. Dust cooling allows fragment masses to reach very small, essentially opacity-limited values of $\gtrsim 10^{-2}M_{\odot}$ (see **Figure 8**). Three-dimensional simulations are needed to determine the ability of a low-metallicity gas to fragment, and to follow the subsequent accretion and merging history of the growing protostars. One such study has been carried out by Clark, Glover & Klessen (2008) who employed a tabulated barotropic equation of state for a low-metallicity gas. The challenge now is to extend such calculations

to realistic initial conditions, and to self-consistently determine the equation of state during the dynamical collapse.

4.4 Radiation from the First Galaxies

4.4.1 IONIZING PHOTON BUDGET AND THE ESCAPE FRACTION First galaxies are promising sources of ultra-violet photons that reionized the intergalactic hydrogen. A critical quantity is the escape fraction of ionizing photons, f_{esc} . Recent simulations that couple the hydrodynamics of the gas in the vicinity of the central star cluster to the continuum radiative transfer of the ionizing radiation from these stars find that the escape fraction strongly evolves with time (Johnson et al. 2009). Initial values are close to zero, when gas densities are still high, and most of the ionizing radiation is bottled up inside the galaxy. With time, however, the photo-ionization heating creates a central high-pressure bubble which in turn drives a strong outflow. Densities thus decrease, until ionizing photons can freely escape into the IGM, leading to a large instantaneous escape fraction of $f_{\text{esc}} \sim 1$. Time-averaged escape fractions are typically quite large, $f_{\text{esc}} \sim 0.1 - 0.8$ (Wise & Cen 2009; Razoumov & Sommer-Larsen 2010). Extinction by a substantial amount of dust can reduce it to $f_{\text{esc}} \sim 0.1$ or less (Gnedin, Kravtsov & Chen 2008; Yajima et al. 2009). Available observations suggest $f_{\text{esc}} < 0.01$ for low-redshift galaxies (e.g., Bridge et al. 2010), whereas $f_{\text{esc}} = 0.01 - 0.1$ for $z \sim 1 - 3$ galaxies (Inoue et al. 2006; Shapley et al. 2006; Siana et al. 2007; Iwata et al. 2009). There are indirect hints from observations of high-redshift galaxies regarding the escape of ionizing radiations, and the stellar populations responsible for this emission (e.g., Jimenez & Haiman 2006).

The ionizing photon budget derived from the currently estimated UV lumi-

nosity function of $z > 6$ galaxies falls short of what is necessary to reionize the Universe (Ouchi et al. 2009). A possible resolution may be either that faint, low-mass galaxies host a substantially “bluer” stellar population, or that the escape fraction from the faint galaxies is actually large. This interpretation of the data agrees with the results from recent cosmological simulations, which consistently predict such large values of f_{esc} .

4.4.2 GLOBAL SIGNATURE The radiation produced by the first galaxies cumulatively contributes to reionization, to the CIB, and to the redshifted 21-cm signal. Here, we only briefly discuss these global signals, as they have been extensively reviewed elsewhere: 21cm cosmology by Furlanetto, Oh & Briggs (2006), Barkana & Loeb (2007), and Morales & Wyithe (2010), the CIB by Hauser & Dwek (2001), Kashlinsky (2005), and Arendt et al. (2010), and reionization in the review papers mentioned in Section 1.

Cosmic reionization imprints distinct large angular-scale patterns in the CMB polarization maps. CMB photons are Thomson-scattered by free electrons in the reionized IGM. As a consequence, the CMB photons are polarized and the temperature fluctuations are damped. These signatures can be used to infer the approximate epoch of reionization. The seven-year *WMAP* data yields the CMB optical depth to Thomson scattering, $\tau \simeq 0.09 \pm 0.03$ (Komatsu et al. 2009), where

$$\tau = \int_0^{z_{\text{reion}}} d\tau_e \approx 0.0023 \left[([1 + z_{\text{reion}}]^3 + 2.7)^{1/2} - 1.93 \right]. \quad (3)$$

for the standard Λ CDM cosmology. Here, we have assumed for simplicity that the IGM is fully ionized at $z < z_{\text{reion}}$. The WMAP measurement provides an integral constraint on the total ionizing photon production at $z > 6$. The contribution from $z < 6$ to the total optical depth amounts only to $\tau \lesssim 0.04$ and thus a

significant volume fraction of the IGM must be ionized to $z = 10$ or higher. Matching the *WMAP* Thomson optical depth constraint provides a non-trivial test for models of early star and galaxy formation. It is unlikely that reionization is completed very early by massive Pop III stars (Cen 2003; Greif & Bromm 2006; Haiman & Bryan 2006). More accurate polarization measurements by the *Planck Surveyor Satellite* will further tighten the constraint on the Thomson optical depth, and in addition might even allow researchers to estimate the reionization history of the Universe (Holder et al. 2003; Mukherjee & Liddle 2008). The latter is usually expressed as the redshift-dependent free electron fraction, $x_e(z)$, which could be much more complex than the simple step function, which is often assumed in approximate interpretations of the data (see Fan, Carilli & Keating 2006).

The first galaxies inevitably contributed to the CIB, through the redshifted Lyman- α recombination line from the HII regions surrounding their stellar sources (Santos, Bromm & Kamionkowski 2002; Salvatera & Ferrara 2003). A vigorous debate has developed around the question of how important still unresolved galaxies at the highest redshifts are, compared to more local, known sources (e.g., Kashlinsky et al. 2005; Thompson et al. 2007). If the difficult subtraction of foreground sources, such as the emission from the interplanetary dust, can be reliably accomplished, a number of key parameters of the first galaxies might be derived from the CIB. One is the typical mass of the first galaxies. In hierarchical structure formation, the mass function is dominated by the lowest mass satisfying the first galaxy criteria (see Section 2). The corresponding dark matter halos then exhibit clustering properties that are characteristic for that mass scale. Those clustering properties are subsequently reflected in the CIB fluctu-

ation power spectrum (Fernandez et al. 2010). A second quantity is the escape fraction of hydrogen ionizing photons from the first galaxies, which could possibly be inferred from the mean intensity of the CIB. The basic idea here is that the production of rest-frame Lyman- α photons is greatly enhanced if the ionizing radiation inside the first galaxies *cannot* escape into the IGM, where densities are very low (recombination lines are emitted at a rate $\propto n^2$). The measured CIB angular power spectrum can largely be attributed to galaxies at $z < 4$, but the possibility for a contribution from $z > 8$ sources still remains (Cooray et al. 2007).

Redshifted 21-cm emission from neutral hydrogen directly probes the topology of reionization (Furlanetto, Oh & Briggs 2006). LOFAR has already begun to collect data and is carrying out its initial calibrations. It will provide statistical information on the distribution of neutral hydrogen at $z \sim 6$, and will eventually be able to map out the distribution directly. Even more powerful is the planned *Square Kilometer Array* (SKA), with an unprecedented sensitivity and spectral coverage. The clustering of the first galaxies can be used to study the topology of reionized regions. If the first galaxies were dominant sources of reionization, their distribution should be anti-correlated with ionized regions that appear as dark holes in 21-cm maps (Lidz et al. 2009).

These global signatures have the advantage that they do not suffer from incompleteness or selection effects of the target galaxies. Very small, faint galaxies that cannot be seen by JWST may in principle leave distinct signatures in the global quantities discussed here.

5 THE FIRST SUPERMASSIVE BLACK HOLES

The origin of SMBHs that power the luminous quasars at high redshifts remains unknown. Spectroscopic observations revealed that BHs with mass greater than 10 billion solar masses were already in place when the age of the universe was less than one billion years (for a review, see Fan, Carilli & Keating 2006). Potentially, the existence of such early SMBHs might pose a challenge to the current cosmological standard model which is based on bottom-up, hierarchical structure formation. The observed SMBHs have likely grown from some smaller seed BHs that were formed earlier, in the progenitors of the luminous quasar host. The first galaxies were plausible sites for seed BH formation, but their own structure and evolution was likely affected by the presence of such early BHs as well. We thus have to tackle a complex, feedback-regulated problem, where our current knowledge is patchy at best.

It is instructive to consider a schematic representation of possible SMBH formation pathways inside the first galaxies (see **Figure 9**). Figure 9 is reproduced from Regan & Haehnelt (2009b), who in turn adopt the well-known flow-chart towards SMBH formation introduced by Rees (1984). The key bifurcation concerns whether the gas inside the first galaxy, here taken to be an atomic cooling halo, can cool below $\sim 10^4$ K or not. Such cooling depends on the presence of either H_2 or heavy-element coolants. To prevent molecular hydrogen from forming, the presence of an extremely strong LW radiation background, capable of photo-dissociating H_2 even in the presence of self shielding would need to be invoked (Bromm & Loeb 2003b; Wise, Turk & Abel 2008; Dijkstra et al. 2008; O’Shea & Norman 2008; Regan & Haehnelt 2009a; Shang, Bryan & Haiman 2010). To maintain metal-free conditions in the first galaxies, star formation and SN ac-

tivity in the progenitor minihalos would have to be suppressed, which may be possible in a subset of cases, in $\sim 10 - 20\%$ of atomic cooling halos collapsing at $z \gtrsim 10$ (Johnson et al. 2008). Below we discuss some of the SMBH formation pathways in greater detail.

5.1 Formation Models

Devising viable models for SMBH formation has been a long-standing challenge in astrophysics (Rees 1984). The requirements on such models are even more stringent in the high-redshift case, where any formation channel has to operate on rapid timescales. There are currently two main ideas, one based on (Pop III) stellar seeds, some of them may grow via gas accretion and BH mergers, and one on the direct collapse of massive primordial gas clouds. Both classes of models face challenges, leaving still open the possibility for alternative, more exotic pathways towards SMBH formation.

5.1.1 POPULATION III STELLAR REMNANTS A popular model assumes that the remnant BHs of Pop III stars seeded the growth of SMBHs (Madau & Rees 2001; Li et al. 2007; Volonteri & Rees 2006; Tanaka & Haiman 2009). In this case, the initial seed mass would be of order $100M_{\odot}$. Given efficient, Eddington-limited accretion, even such low-mass seeds could readily grow to the SMBHs inferred to power the high- z SDSS quasars in the roughly 500 Myr between seed formation and $z \sim 6$ (Haiman & Loeb 2001). Recent studies suggest, however, that the gas accretion onto early BHs is inefficient until the BHs are incorporated into larger mass halos. One impeding effect is that the gas is already evacuated by photoionization heating from the progenitor massive star (Kitayama et al. 2004; Whalen et al. 2004; Alvarez, Bromm & Shapiro 2006; Abel, Wise & Bryan 2007).

After the progenitor star has died and directly collapsed into an intermediate mass BH, it thus finds itself in a very low-density region. Accretion rates are then negligible for at least the free-fall time of the dark matter host systems (Johnson & Bromm 2007; Pelupessy, Di Matteo & Ciardi 2007; Alvarez, Wise & Abel 2009). In addition, the radiative feedback from the accreting BH can reduce the cooling of the surrounding gas, e.g., by photo-dissociating H_2 , thus further reducing accretion. Even if the gas supply in the vicinity of the remnant BH has been replenished, accretion likely continues to be severely suppressed compared to the Eddington rate. This is because of radiation pressure on the high-density infalling gas (Milosavljevic et al. 2009a,b). As a result, an episodic, quasi-periodic accretion flow is established, with a time-average significantly below the Bondi-Hoyle and Eddington rates (see **Figure 10**).

This early bottleneck for growing the seeds to SMBHs poses a serious challenge to the Pop III stellar remnant scenario. However, it is important to note that the emergence of SMBHs should not be too common, to be compatible with the abundance of observed luminous quasars (Tanaka & Haiman 2009). It is not necessary that a particular process is able to feed all seed BHs efficiently, although there must be at least one physical mechanism that enables the early formation of SMBHs perhaps under some extraordinary conditions. Models that invoke special conditions such as super-Eddington growth in accretion disks might therefore be acceptable solutions to the early bottleneck problem.

5.1.2 DIRECT COLLAPSE The early bottleneck to growth described above arises because of the negative feedback from star formation. In principle, the same is true for the rapid collapse of more massive clouds (Loeb & Rasio 1994; Eisenstein & Loeb 1995). However, there is again an intriguing possibility in atomic

cooling halos. If H_2 and metal cooling were suppressed, atomic hydrogen cooling could still allow the gas to collapse into the halo with $T_{\text{vir}} \sim 10^4$ K. But due to the absence of lower temperature coolants, the collapse would proceed isothermally without any sub-fragmentation, and therefore without star formation. Recently, the atomic cooling halo pathway has received considerable attentions, both from the simulation side (Bromm & Loeb 2003b; Wise, Turk & Abel 2008; Regan & Haehnelt 2009a; Johnson et al. 2010; Latif, Zaroubi & Spaans 2011; Shang, Bryan & Haiman 2010), and with analytical work (Begelman, Volonteri & Rees 2006; Lodato & Natarajan 2006, 2007; Spaans & Silk 2006). The key question is whether the gas can indeed remain free of H_2 molecules (Dijkstra et al. 2008; Ahn et al. 2009), and of metals (Johnson, Greif & Bromm 2008; Omukai, Schneider & Haiman 2008). Again, it is important to remember that such a mechanism, where already more massive seed BHs with $\gtrsim 10^4 M_\odot$ form via direct collapse of a primordial gas cloud, needs to successfully operate only in a few, rare cases. Indeed, if *every* atomic cooling halo were to produce a massive seed BH in its center at $z \gtrsim 10$, we would exceed the locally measured total BH mass density (e.g., Yu & Tremaine 2002). Fragmentation may also be suppressed by the strong turbulence in inflows with high Mach number, where gas temperatures are significantly *below* the virial temperature (Begelman & Shlosman 2009). This scenario still needs to be tested, however, with realistic simulations. Recently, a qualitatively different variant of massive seed BH formation during direct collapse has been suggested (Mayer et al. 2010). In this model, two very massive ($\sim 10^{13} M_\odot$) halos merge at high redshifts, triggering massive inflows into the center of the ensuing potential well on such a rapid timescale that negative feedback from star formation has no opportunity to interfere with the BH assembly process. It is not entirely clear,

however, whether such a set-up will occur in a realistic cosmological setting.

5.1.3 OTHER MODELS Overall, there appears to remain a large uncertainty in these models. The Pop III seed model requires a number of optimistic assumptions on the efficiency of gas accretion and multiple BH mergers, whereas the rapid collapse model critically relies on the assumption that a massive BH does indeed form in a hot, dense gas cloud. Alternative models for SMBH formation have also been proposed recently. Primordial stars powered by dark matter annihilation (Spolyar et al. 2008; Iocco et al. 2008; Umeda et al. 2009) are suggested to have long lifetimes, because they do not consume hydrogen by nuclear burning. If such objects continued to accrete the surrounding gas, they could grow to become more massive than $10^5 M_{\odot}$. Such very massive “dark stars” can be as luminous as $\sim 10^{10} L_{\odot}$, in principle detectable with *JWST* (Freese et al. 2010), and they can also collapse to massive BHs at their death.

5.2 SMBH-First Galaxy Coevolution

It is well-known that in the local Universe, there is a tight correlation between the bulge properties of a galaxy and the mass of its central BH (Gebhardt et al. 2000; Ferrarese & Merritt 2000). Whether or not the same relationship holds in the young Universe is an intriguing question. Volonteri & Natarajan (2009) argue that a similar relationship can be quickly established, and that it would be mainly driven by accretion onto BHs after major mergers of the host galaxies. Coevolution of the first galaxies and early BHs might be a key in shaping the high-redshift galaxies, as has been advocated for somewhat lower-redshift galaxies (Di Matteo, Springel & Hernquist 2005). The detailed study of the star-formation history of $z > 6$ galaxies might provide clues as to whether star formation was

episodic, both within themselves and in their progenitor systems (e.g., Labbe et al. 2010).

6 *James Webb Space Telescope* SIGNATURE

The upcoming *JWST*, together with the next-generation of 30-40m extremely large ground-based telescopes, will revolutionize our picture of the high-redshift Universe. Among the main *JWST* science goals is the detection of light from the first galaxies, and more generally to elucidate early structure formation at the end of the cosmic dark ages (Gardner et al. 2006). The key predictions concern the expected flux and number densities of the first galaxies, enabling us to assess their detectability with the instruments aboard the *JWST* (e.g., Salvaterra, Ferrara & Dayal 2011). In carrying out these predictions, a number of challenges still need to be overcome prior to its projected launch in ~ 2015 (see the contributions in Whalen, Bromm & Yoshida 2010). We begin by briefly summarizing the *JWST* capabilities. A more detailed discussion is made by Gardner et al. (2006) and Stiavelli (2009).

6.1 *JWST* Instruments and Sensitivities

The observatory will carry out deep field imaging with the Near-Infrared Camera (NIRCam) and the Mid-Infrared Instrument (MIRI), as well as medium-resolution spectroscopy with the Near-Infrared Spectrograph (NIRSpec) and MIRI. NIRCam will have a field of view of $2.2' \times 4.4'$, and an angular resolution of $\sim 0.03'' - 0.06''$ in the range of observed wavelengths $\lambda_{\text{obs}} = 0.6 - 5\mu\text{m}$. The multi-object spectrograph NIRSpec will carry out medium resolution ($R \sim 100 - 3000$) spectroscopy of up to ~ 100 objects simultaneously within a field of view of

$3.4' \times 3.4'$, where $R \equiv \lambda_{\text{obs}}/\Delta\lambda_{\text{obs}}$ is the spectral resolution. NIRSpec will operate in the same wavelength range as NIRCам but at lower angular resolution ($\sim 0.1''$). Finally, MIRI will complement NIRCам and NIRSpec by providing imaging, low and medium resolution spectroscopy within the range of observed wavelengths $\lambda_{\text{obs}} = 5 - 28.8\mu\text{m}$ and fields of view and angular resolutions of, respectively, $\sim 2' \times 2'$ and $\sim 0.1'' - 0.6''$.

In quoting sensitivities, or flux limits f_{lim} , for the *JWST* instruments, a signal-to-noise ratio of $S/N = 10$ and exposure times of $t_{\text{exp}} = 10^4$ s are often assumed. These baseline sensitivities are summarized in table 10 by Gardner et al. (2006). Ultra-deep exposures with *JWST* may extend to $t_{\text{exp}} = 10^6$ s, which is comparable to the HUDF observations, with flux limits being rescaled according to: $f_{\text{lim}} \propto 1/\sqrt{t_{\text{exp}}}$. Panagia (2005) contains a useful graphical representation of the *JWST* sensitivities, nicely emphasizing the jump in going from the near-IR to the mid-IR. Approximate numbers, for the deep exposures, are $f_{\text{lim}} \sim 1$ nJy for NIRCам, and 10 times higher for the MIRI imager; spectroscopic limits are typically two orders of magnitude higher than the imaging ones. It is customary to also work with the AB magnitude system (Oke 1974; Oke & Gunn 1983). Specific fluxes, f_{ν} , can then be expressed as

$$m_{\text{AB}} = -2.5 \log_{10} \left(\frac{f_{\nu}}{\text{nJy}} \right) + 31.4. \quad (4)$$

Even for exposure times as long as 10^6 s, *JWST* will not have sufficient sensitivity to detect sources with stellar masses below $\sim 10^5 - 10^6 M_{\odot}$. In particular, *JWST* will not be able to directly detect individual Pop III stars at high redshifts (Bromm, Kudritzki & Loeb 2001). Therefore, starbursts in the first galaxies are the primary targets for *JWST*. As was already recognized by Partridge & Pee-

bles (1967), the first galaxies were likely brightest in the recombination lines of hydrogen and helium (Schaerer 2002, 2003; Johnson et al. 2009; Pawlik, Milosavljevic & Bromm 2011), in particular the Lyman- α , H α and He II 1640 Å nebular emission lines (see **Figure 11**).

The flux from the redshifted He II 1640 Å line ($\lambda_{\text{em}} = 1640 \text{ \AA}$), as well as the flux from the redshifted Ly α line ($\lambda_{\text{em}} = 1216 \text{ \AA}$), would be detected by *JWST* with NIRSpec at a spectral resolution of $R \sim 1000$, whereas the redshifted H α line ($\lambda_{\text{em}} = 6563 \text{ \AA}$) would be detected with MIRI at a spectral resolution $R \sim 3000$. Finally, the redshifted (soft) UV continuum, at $\lambda_{\text{em}} = 1500 \text{ \AA}$, would be detected using NIRCам.

6.2 Observing High-redshift Sources

It is convenient to review the basic relations that relate observed to intrinsic quantities, as employed in observational cosmology (see also Loeb 2010).

We begin by translating intrinsic line and UV continuum luminosities into observed fluxes. The specific flux from a spatially unresolved object emitted in a spectrally unresolved line with rest-frame wavelength λ_{em} and intrinsic line luminosity L_{em} is given by Oh (1999) and Johnson et al. (2009):

$$f(\lambda_{\text{obs}}) = \frac{L_{\text{em}}}{4\pi d_L^2(z)} \frac{1}{\Delta\nu_{\text{obs}}}, \quad (5)$$

where $\Delta\nu_{\text{obs}} = c/(\lambda_{\text{obs}}R)$, and $\lambda_{\text{obs}} = (1+z)\lambda_{\text{em}}$. A convenient approximation for the luminosity distance is: $d_L \sim 100[(1+z)/10] \text{ Gpc}$. For typical parameters, one then has:

$$f(\lambda_{\text{obs}}) \simeq 3 \text{ nJy} \left(\frac{L_{\text{em}}}{10^{40} \text{ erg s}^{-1}} \right) \left(\frac{\lambda_{\text{em}}}{1216 \text{ \AA}} \right) \left(\frac{R}{1000} \right) \left(\frac{1+z}{11} \right)^{-1}.$$

Let us now discuss whether the lines, expected to be emitted by the first galaxies, are indeed spatially and spectrally unresolved. The assumption of spectrally unresolved lines is excellent for both $\text{H}\alpha$ and $\text{He II } 1640 \text{ \AA}$, whose line widths $\Delta\lambda/\lambda < 10^{-4}(T/10^4\text{K})^{1/2}$ are set by thermal Doppler broadening at temperature $T < 10^4 \text{ K}$ (Oh 1999). At redshifts $z \gtrsim 10$ a transverse physical scale Δl corresponds to an observed angle $\Delta\theta = \Delta l/d_A \sim 0.1''(\Delta l/0.5\text{kpc})[(1+z)/10]$, where $d_A = (1+z)^{-2}d_L$ is the angular diameter distance. If the recombination lines originate in the ionized nebulae in the central regions of the first galaxies at $r < 0.1r_{\text{vir}}$, the assumption that the emitting regions are spatially unresolved is also good for both the $\text{H}\alpha$ and the $\text{He II } 1640 \text{ \AA}$ lines, and it applies equally well to the UV continuum. Here, we use a virial radius of $r_{\text{vir}} \sim 1 \text{ kpc}$ to describe the overall size of the first galaxies, which is typical for the systems discussed in Section 4. In contrast, the Lyman- α line undergoes resonant scattering (Harrington 1973; Neufeld 1990), and hence will originate from within a spatially extended region with typical angular size $\Delta\theta \sim 15''$ (Loeb & Rybicki 1999), and be heavily damped due to absorption by intergalactic neutral hydrogen (Santos 2004; but see Dijkstra & Wyithe 2010). Indeed, Lyman- α radiation from galaxies at redshifts $z \gtrsim 10$ may be severely attenuated because the bulk of the Universe was likely still substantially neutral at these redshifts.

A complementary way to quantify the strength of an observed line uses (redshifted) equivalent widths, which can easily be translated into the corresponding rest-frame values (e.g., Johnson et al. 2009): $W_0 = f_{\text{line}}/f_\lambda$, where we have used the intrinsic line and neighboring (specific) UV continuum fluxes. Predicted equivalent widths for the first galaxies can reach $W_0 \gtrsim 100 \text{ \AA}$ for $\text{He II } 1640 \text{ \AA}$, and $W_0 \gtrsim 100 \text{ \AA}$ for the hydrogen lines (Johnson et al. 2009).

6.3 Modelling Star Formation in the First Galaxies

Making predictions for the luminosities and colors of the first galaxies sensitively depends on what one assumes for the stellar populations and star formation model (e.g., Schaerer 2002, 2003; Johnson et al. 2009; Raiter, Schaerer & Fosbury 2010; Pawlik, Milosavljevic & Bromm 2011; Salvaterra, Ferrara & Dayal 2011). One possibility is that stars form in a single instantaneous burst with total stellar mass

$$M_{\star} \sim 10^5 M_{\odot} \left(\frac{f_{\star}}{0.1} \right) \left(\frac{f_{\text{cool}}}{0.01} \right) \left(\frac{M_{\text{vir}}}{10^8 M_{\odot}} \right), \quad (6)$$

where f_{cool} is a conversion factor that determines the amount of gas mass available for starbursts inside halos with virial masses M_{vir} , and f_{\star} is the star-formation efficiency, i.e., the fraction of the available gas mass that is turned into stars. The parameters are normalized to what we have learned from simulating the formation of atomic cooling halos (see Section 4). Specifically, the choice of $f_{\text{cool}} = 0.01$ reflects the rapid accretion ($t_{\text{acc}} < 10$ Myr) of large gas masses ($M_{\text{gas}} > 10^6 M_{\odot}$) into the central regions, as seen in the simulations. The star formation efficiency may be quite high in a burst mode, $f_{\star} = 0.1$, where accretion times are comparable to the typical lifetimes (~ 10 Myr) of massive stars. Star formation may then not be affected by strong feedback capable of halting the collapse of the accreting gas. Another possibility is that stars form continuously. Atomic cooling halos, with their masses of $\sim 10^8 M_{\odot}$, may have potential wells that are still too shallow to enable continuous star formation despite the disruptive effects of stellar feedback (see Section 4). Galaxies with total (virial) masses of $\gtrsim 10^9 M_{\odot}$, however, may have been able to sustain such a near-continuous mode (Wise & Cen 2009). One can approximately include the effect of stellar feedback

by employing a lower efficiency, $f_{\star} = 0.01$, than appropriate for a starburst. The implied star formation rates $\dot{M}_{\star}(z) \sim 0.1M_{\odot} \text{ yr}^{-1}$ are consistent with those found in recent low-mass galaxy formation simulations (Wise & Cen 2009; Razoumov & Sommer-Larsen 2010).

The luminosities of the first galaxies critically depend on the metallicities, ages, and IMF of their stellar populations. Some of the lowest-mass galaxies may still contain zero-metallicity gas. The resulting stars may form with a top-heavy IMF, biased towards high mass ($M_{\star} \sim 100M_{\odot}$) stars, as is expected to be the case for the first, metal-free generation of stars which form via molecular hydrogen cooling (Bromm et al. 2009). The IMF of metal-free stars is, however, still subject to large theoretical uncertainties. Stars forming out of gas with elevated electron fractions, such as produced behind structure formation or SN shocks, or as present in ionized regions, could have characteristic masses substantially less than $< 100M_{\odot}$ (see Section 4). The assumption of metal-free star formation will be violated if previous episodes of star formation, for instance inside the progenitors of the assembling galaxy, enriched the gas with metals. Even a modest enrichment to critical metallicities as low as $Z_{\text{crit}} < 10^{-6} - 10^{-3.5}Z_{\odot}$ may imply the transition from a top-heavy IMF to a normal IMF (Bromm et al. 2001; Santoro & Shull 2006; Schneider et al. 2006; Smith & Sigurdsson 2007). Note that even a few SN explosions may already be sufficient to enrich low-mass ($\sim 10^8M_{\odot}$) galaxies to metallicities $Z > Z_{\text{crit}}$ (Wise & Abel 2008; Karlsson, Johnson & Bromm 2008; Greif et al. 2010; Maio et al. 2011).

The luminosity in the He II 1640 Å line strongly depends on both the IMF and stellar metallicity, and also on the age of the galaxy, i.e., the time since the last major star-formation episode. At fixed IMF, a change from low to zero metallicity

implies an increase in the He II 1640 Å line luminosity by about three orders of magnitude for the first few million years after the starburst. This reflects the exceptionally hot atmospheres of zero-metallicity stars that render them into strong emitters of He II ionizing radiation (Tumlinson & Shull 2000; Bromm, Kudritzki & Loeb 2001; Schaerer 2003). For a top-heavy IMF, as advocated for primordial or very low-metallicity stars, the line luminosity is increased by another order of magnitude (see **Figure 12**). The large differences in luminosities offer the prospect of distinguishing observationally between stellar populations consisting of metal-free or metal-enriched stars, and of constraining their IMFs (Tumlinson & Shull 2000; Bromm, Kudritzki & Loeb 2001; Oh 2001; Johnson et al. 2009). *JWST* has the potential to constrain the properties of starbursts in galaxies with halo masses as low as $\sim 10^9 M_\odot$, based on the simultaneous detection/non-detection of the H α and He II 1640 Å lines (Pawlik, Milosavljevic & Bromm 2011). Indeed, only zero-metallicity starbursts with a top-heavy IMF can be detected in both H α and He II 1640 Å, assuming exposure times $\lesssim 10^6$ s. Whether Lyman- α can be detected as well will depend on the attenuation due to resonant scattering in the neutral IGM. Because of the greater sensitivity of NIRSpec compared to MIRI, Lyman- α line emission is potentially easier to detect than H α , and it hence remains a very powerful probe of galaxy formation at redshifts $z \gtrsim 10$, despite the large uncertainties caused by its resonant nature.

6.4 Source Number Counts

The second key prediction concerns the number density of the first galaxies that *JWST* may observe. We can estimate the number of galaxies detectable with *JWST*, per unit solid angle, above redshift z as follows (e.g., Pawlik, Milosavljevic

& Bromm 2011):

$$\frac{dN}{d\Omega}(> z) = \int_z^\infty dz' \frac{dV}{dz'd\Omega} \frac{\tau_{\text{sb}}}{t_{\text{H}}(z')} \int_{M_{\text{min}}(z')}^\infty dM n(M, z'), \quad (7)$$

where $t_{\text{H}}(z)$ is the age of the Universe at z , and

$$\frac{dV}{dzd\Omega} = \frac{cd_{\text{L}}^2}{1+z} \left| \frac{dt}{dz} \right|$$

the comoving volume element per unit solid angle and redshift. Here $|dt/dz|^{-1} \simeq (1+z)H_0\Omega_{\text{m}}^{1/2}(1+z)^{3/2}$, valid for high redshifts. $n(M, z)$ is the comoving number density of galaxy host halos with mass M at redshift z , which can be derived from large cosmological simulations, or calculated with approximate analytical techniques. The latter approach often relies on variants of the Press-Schechter formalism (Press & Schechter 1974; for a recent review, see Zentner 2007). $M_{\text{min}}(z)$ is the lowest (total or virial) halo mass capable of hosting a starburst that can be detected by the *JWST*. It depends on the stellar properties (metallicity and IMF), and on whether observations are made in, e.g., the $\text{H}\alpha$ line, the He II 1640 Å line, or in the soft continuum. Typical values are $M_{\text{min}} \sim 10^8 - 10^9 M_{\odot}$ for $z \simeq 10 - 15$ (Pawlik, Milosavljevic & Bromm 2011). Finally, τ_{sb} gives the duration of the starburst, which may vary from ~ 3 Myr for top-heavy Pop III stars, to ten times larger values for stars with normal IMF. In each case, this timescale measures the approximate time after which negative stellar feedback terminates the starburst. In **Figure 13**, we show results from a Press-Schechter based calculation (Pawlik, Milosavljevic & Bromm 2011), demonstrating that *JWST* may detect a few tens (for $Z > 0$ and normal IMF) up to a thousand (for Pop III with a top-heavy IMF) starbursts from $z > 10$ in its field-of-view of ~ 10 arcmin². This estimate is consistent with previous studies for similar assumptions about the conversion

between halo and stellar mass (e.g., Haiman & Loeb 1997, 1998; Oh 1999; Trenti & Stiavelli 2008). Current calculations, however, still suffer from a number of uncertainties, such as whether Case B recombination theory is appropriate in the first galaxies (Schaerer 2003; Raiter, Schaerer & Fosbury 2010), the role of dust extinction (Trenti & Stiavelli 2006), the feedback-regulated star formation efficiency, and the escape fraction of ionizing radiation (Gnedin, Kravtsov & Chen 2008; Wise & Cen 2009; Johnson et al. 2009; Razoumov & Sommer-Larsen 2010; Yajima, Choi & Nagamine 2011).

7 STELLAR ARCHAEOLOGY

Stellar Archaeology is the endeavor to constrain the properties of the first stars by scrutinizing the chemical abundance patterns in the most metal-poor, and therefore presumably oldest, stars in the Milky Way and nearby galaxies within the Local Group (Beers & Christlieb 2005; Frebel 2010). Such a near-field cosmological approach nicely complements the traditional far-field cosmology based on high-redshift observations (Freeman & Bland-Hawthorn 2002). The first galaxies may have left behind a number of local fossils as well. *(i)* Some of the numerous dwarf galaxies in the Local Group may constitute the survivors of the first galaxies. In this regard, the ultra-faint dwarf (UFD) galaxies, recently discovered in the SDSS, are of particular promise. *(ii)* The first galaxies likely were the formation sites for the first low-mass Pop II stars (e.g., Tumlinson 2010). These eventually found their way into the halo, and possibly bulge, of our Galaxy through its complex hierarchical assembly process. *(iii)* Finally, a subset of the first galaxies may have provided the birth places for old, metal-poor globular clusters (GCs), which again might have been incorporated into our MW (Bromm & Clarke 2002;

Kravtsov & Gnedin 2005; Brodie & Strader 2006; Boley et al. 2009). We focus on the first issue, as it is of most direct relevance for this review.

7.1 Ultrafaint Dwarf Galaxies

The newly discovered UFD galaxies are the intrinsically least luminous members ($L_{\text{tot}} \lesssim 10^5 L_{\odot}$) of the Local Group (Kirby et al. 2008; Martin, de Jong & Rix 2008). Due to their simple assembly history, they can be regarded as the closest local relatives to the first galaxies. They are believed to have had only one or few early star formation events, but have been quiescent ever since (Tolstoy, Hill & Tosi 2009). Hence, they should reflect the signatures of the earliest stages of chemical enrichment in their population of low-mass stars. As opposed to the MW halo, which was assembled through numerous merger and accretion events, the lowest luminosity dwarfs provide us with a much cleaner fossil record of early star and galaxy formation. With their small number of stars (of order a few hundred), the UFDs may allow us to carry out a virtually complete census of their stellar content (Simon et al. 2011). Medium-resolution spectroscopic studies have shown that all of the UFDs have large $[\text{Fe}/\text{H}]$ spreads of ~ 1 dex or more (Kirby et al. 2008; Norris et al. 2010), reaching below $[\text{Fe}/\text{H}] = -3.0$. Moreover, some of them have average metallicities as low as $\langle [\text{Fe}/\text{H}] \rangle \sim -2.6$, which is lower than the values found in the most metal-poor GCs. The abundances of dwarf galaxy stars closely resemble those found in similarly metal-poor Galactic halo stars. Overall, this suggests that chemical evolution proceeded very similarly at the early times which are probed with the most metal-poor, and thus presumably the oldest, stars in a given system (Frebel & Bromm 2011). The same chemical behavior has also been found in Sculptor, a more luminous, classical dwarf spheroidal (dSph)

galaxy, at $[\text{Fe}/\text{H}] \sim -3.8$ (Frebel et al. 2010). However, at higher metallicity ($[\text{Fe}/\text{H}] > \sim -2.5$), the Sculptor stellar ($[\alpha/\text{Fe}]$ -) abundances deviate with respect to the behavior of Galactic halo stars (Geisler et al. 2005), indicating a different evolutionary timescale and multiple star-formation events (Tolstoy et al. 2004).

7.2 Theoretical Models

There is widespread consensus that the UFDs may provide us with the *Rosetta Stone* for galaxy formation, given their relative simplicity. It is therefore very tempting to theoretically model their formation process. When did they form, and how do they fit into the hierarchical Λ CDM cosmology? What kind of star formation history did they experience, and, related to this, how many SNe did contribute to their complement of metals? This field is still very young, and it is likely that progress over the next few years will be rapid. Here, we only provide a few comments to illustrate the flavor of the developing argument.

7.2.1 FORMATION SITE Currently, two main ideas for the origin of the UFDs are discussed in the literature. One class of models invokes H_2 -cooling minihalos (Bovill & Ricotti 2009, 2011; Salvadori & Ferrara 2009). The models couple a representation of the evolving dark matter distribution, either from cosmological simulations or from Press-Schechter type techniques, with a recipe for star formation and feedback, and can successfully explain the broad observational properties of the UFD population (see **Figure 14**). The suggested antecedents of the UFDs would then have been minihalos with masses $M \simeq 10^7 - 10^8 M_\odot$, close to the threshold where atomic cooling sets in. A challenge for these models comes from the highly-resolved, ab initio simulations discussed in Section 4. The underlying question again is where second-generation star formation can occur,

already in minihalos or only in the next stage of hierarchical assembly, the atomic cooling halos (see the discussion in Section 2). Within the minihalo scenario, the same system would have to first lead to the explosion of Pop III SNe, subsequently reassemble the enriched gas inside their shallow potential well despite strong negative feedback effects, and finally trigger a second generation of star formation. The strength of the negative feedback crucially depends on the Pop III IMF; the more top-heavy it is, the longer the delay time between first and second generation star formation. For the minihalo model as UFD progenitors to work, one has to assume that the first stars typically were not too massive.

The above challenge provides the motivation for the competing model to explain the origin of UFDs (Maccio et al. 2010; Frebel & Bromm 2011). In the atomic cooling halo pathway, the sites for first and second-generation star formation are decoupled (see **Figure 1**), thus alleviating the problem of admitting local Pop III pre-enrichment.

7.2.2 ENRICHMENT MODE An important clue to the true nature of the UFD formation site could come from a knowledge of the chemical enrichment mode. Did enrichment in the UFD progenitors occur in one initial burst, to be completely shut-off subsequently, or continuously, spread out over an extended star formation and SN history? The first possibility has been termed “one-shot” chemical enrichment by Frebel & Bromm (2011). The answer to this question would provide us with important clues about the strength of the feedback in the first galaxies. If this feedback was sufficiently violent to disrupt the first galaxy already after its initial starburst, blowing all remaining gas into the general IGM, “one-shot” conditions would be realized. The simulations have not yet answered this question with any degree of certainty, but one can look for the chemical

signature of such burst-like enrichment in the stellar content of the UFDs (Frebel & Bromm 2011). Their surviving Pop II stars would then preserve the yields from the initial Pop III SNe that had occurred in the progenitor minihaloes without any subsequent enrichment from events that operated on timescales longer than the short dynamical time that governs the formation of the starburst, such as type Ia SNe or AGB winds. Specifically, one would expect high $[\alpha/\text{Fe}]$ values for *all* stars in the UFD, and low n-capture abundances due to the absence of any s-process contribution from AGB stars.

An important caveat is that a subset of those Pop II stars might have experienced post-processing of their surface abundance, e.g., via mass transfer from a binary companion or dredge-up events during later stages of stellar evolution. A possible strategy to circumvent this problem is to realize that almost all stars form in clusters. A properly defined multi-dimensional abundance space could thus uniquely identify the primordial signature through this clustering effect (Bland-Hawthorn et al. 2010).

7.2.3 LESSONS LEARNED Currently, the lowest luminosity dwarfs are consistent with the one-shot criteria, but the data is still very sparse, and the case therefore remains inconclusive. The hope is that high-resolution spectroscopy of more UFD stars will soon become available. The abundance ratios in most individual stars reflect an enrichment history that is dominated by core-collapse SNe, even in the higher metallicity regime ($[\text{Fe}/\text{H}] \sim -2.0$). The latter is dominated by SNIa enrichment in the more luminous classical dSphs. The observed spread in Fe and other elements may suggest that mixing in the UFD progenitors was not very efficient, at least on scales of $\gtrsim 10$ pc, whereas mixing on smaller scales may have been almost complete, if the simulations discussed in Section 4

are correct. The suggested signature from clustered star formation in the first galaxies may again help to constrain the mixing efficiency on different length scales (Bland-Hawthorn et al. 2010). Without inhomogeneous mixing, all stars should have nearly identical abundances, similar to what is found in globular cluster. We can thus tentatively infer that GCs must have formed in more massive haloes where turbulent mixing would have been much more efficient.

As additional abundances of individual dwarf galaxy stars become available, abundance gradient studies of the UFD galaxies should shed further light on the mixing efficiency. Stronger gravitational fields in the center of a system would drive more turbulence that in turn would induce mixing. Because the UFDs are ideal testbeds for various feedback processes, it will also be interesting to study the carbon abundances in these systems. Carbon, as well as oxygen, may have been a key cooling agent inside the first galaxies (Bromm & Loeb 2003a). Although one extremely carbon-rich star (with $[\text{Fe}/\text{H}] \sim -3.5$) has recently been found in Segue 1 (Norris et al. 2010a), low stellar C abundances, if ever found, would greatly weaken the theory of fine-structure line cooling for driving the transition to low-mass star formation.

8 OUTLOOK

The most crucial immediate challenge, for both observers and theorists, is to close the gap between the mass scale accessible to ab initio simulations (virial masses of $\sim 10^8 M_\odot$), and to cutting-edge observations (inferred total masses of $\sim 10^{10} M_\odot$). We have encountered this fundamental problem repeatedly in our preceding discussion. A second key need is to derive better predictions for the number counts of the first galaxies, and to devise robust multi-color and spectro-

scopic criteria to disentangle the likely mix of Pop III and Pop II stars, possibly together with an AGN component, encountered in the first galaxies. The appearance of the first galaxies in sub-millimeter to radio bands needs to be explored theoretically. In particular, atomic and molecular lines such as CII and CO lines may be promising in detecting and characterizing the first galaxies (Walter & Carilli 2007; Obreschkow et al. 2009). Finally, to fully harness the tremendous potential of stellar archaeology in local dwarf galaxies, a much increased sample of high-quality elemental abundances is needed.

The study of the first galaxies enters an exciting period, where advances in supercomputer technology enable ever more realistic ab initio simulations within a realistic cosmological context. This is matched by equally exciting prospects on the observational side, where next-generation facilities – such as *JWST*, the planned 30-40m extremely large telescopes on the ground, ALMA, and the SKA – will finally open up the high-redshift frontier. It is very likely that if another review on the first galaxies is written a decade from now, our understanding of the subject will have completely changed. This again reflects the special stage this field is in, where we are just at the threshold of a golden age of discovery.

ACKNOWLEDGMENTS

The authors thank Andrew Benson, Andrea Ferrara, Zoltan Haiman, Adam Lidz, Masami Ouchi, and John Wise for carefully reading earlier drafts of the present review and also for providing comments. V.B. is supported by the National Science Foundation grant AST-1009928, and by NASA through Astrophysics Theory and Fundamental Physics Program grants NNX08-AL43G and NNX09-AJ33G. N.Y. acknowledges support from the Grants-in-Aid for Young Scientists

(S) 20674003 by the Japan Society for the Promotion of Science and from World Premier International Research Center Initiative (WPI Initiative), MEXT, Japan.

LITERATURE CITED

- Abel T, Wise JH, Bryan GL. 2007. *Ap. J.* 659:L87-90
- Ahn K, Shapiro PR. 2007. *MNRAS* 375:881-908
- Ahn K, Shapiro PR, Iliev IT, Mellema G, Pen UL. 2009. *Ap. J.* 695:1430-45
- Alvarez MA, Bromm V, Shapiro PR. 2006. *Ap. J.* 639:621-32
- Alvarez MA, Wise JH, Abel T. 2009. *Ap. J.* 701:L133-137
- Arendt RG, Kashlinsky A, Moseley SH, Mather J. 2010. *Ap. J. Suppl.* 186:10-47
- Barkana R, Loeb A. 2001. *Phys. Rep.* 349:125-238
- Barkana R, Loeb A. 2007. *Rep. Prog. Phys.* 70:627-57
- Becker GD, Rauch M, Sargent WLW. 2009. *Ap. J.* 698:1010-19
- Begelman M, Shlosman I. 2009. *Ap. J. Lett.* 702:L5-8
- Begelman M, Volonteri M, Rees MJ. 2006. *Ap. J.* 370:289-298
- Beers TC, Christlieb N. 2005. *Annu. Rev. Astron. Astrophys.* 43:531-80
- Begelman M, Shlosman I. 2009. *Ap. J. Lett.* 702:L5-8
- Begelman M, Volonteri M, Rees M. 2006 *Ap. J.* 370:289-98
- Benson A. 2010. *Phys. Rep.* 495:33-86
- Bertone S, Stoehr F, White SDM. 2005. *MNRAS* 359:1201-16
- Bland-Hawthorn J, Karlsson T, Sharma S, Krumholz M, Silk J. 2010. *Ap. J.* 721:582-96
- Blumenthal GR, Faber SM, Primack JR, Rees MJ. 1984. *Nature* 311:517-25
- Boley AC, Lake G, Read J, Teyssier R. 2009. *Ap. J. Lett.* 706:L192-96
- Bouwens RJ, Illingworth GD, Gonzalez V, Labbe I, Franx M, et al. 2010a. *Ap.*

J. 725:1587-99

Bouwens RJ, Illingworth GD, Oesch PA, Stiavelli M, van Dokkum P, et al. 2010b.

Ap. J. Lett. 709:L133-36

Bouwens RJ, Illingworth GD, Oesch PA, Trenti M, Stiavelli M, et al. 2010c. *Ap.*

J. Lett. 708:L69-72

Bouwens RJ, Illingworth GD, Labbe I, Oesch PA, Trenti M, et al. 2011. *Nature*

469:504-7

Bovill MS, Ricotti M. 2009. *Ap. J.* 693:1859-70

Bovill MS, Ricotti M. 2011. *Ap. J.* Submitted (arXiv:1010.2231)

Bridge CR, Teplitz HL, Siana B, Scarlata C, Conselice CJ, et al. 2010. *Ap. J.*

720:465-79

Brodie JP, Strader J. 2006. *Annu. Rev. Astron. Astrophys.* 44:193-267

Bromm V, Clarke CJ. 2002. *Ap. J. Lett.* 566:L1-4

Bromm V., Kudritzki RP, Loeb A. 2001. *Ap. J.* 552:464-72

Bromm V, Larson RB. 2004. *Annu. Rev. Astron. Astrophys.* 42:79-118

Bromm V., Loeb A. 2003a. *Nature* 425:812-14

Bromm V., Loeb A. 2003b. *Ap. J.* 596:34-46

Bromm V, Ferrara A, Coppi PS, Larson RB. 2001. *MNRAS* 328:969-76

Bromm V, Yoshida N, Hernquist L. 2003. *Ap. J. Lett.* 596:L135-38

Bromm V, Yoshida N, Hernquist L, McKee CF. 2009. *Nature* 459:49-54

Bryan GL, Norman ML. 1998. *Ap. J.* 495:80-99

Castellano M, Fontana A, Paris D, Grazian A, Pentericci L, et al. 2010. *Astron.*

Astrophys., 524:28

Cattaneo A, Faber SM, Binney J, Dekel A, Kormendy J. 2009. *Nature* 460:213-19

Cazaux S, Spaans M. 2009. *Astron. Astrophys.* 496:365-74

- Cen R. 2003. *Ap. J.* 591:12-37
- Ciardi B, Ferrara A. 2005. *Space Sci. Rev.* 116:625-705
- Clark PC, Glover SCO, Klessen RS. 2008. *Ap. J.* 672:757-64
- Clark PC, Glover SCO, Klessen RS, Bromm V. 2011. *Ap. J.* 727:110
- Cooper AP, Cole S, Frenk CS, White SDM, Helly J, et al. 2010. *MNRAS* 406:744-66
- Cooray A, Sullivan I, Chary RR, Bock JJ, Dickinson M, et al. 2007. *Ap. J. Lett.* 659:L91-94
- Choudhury RT, Ferrara A. 2006. *MNRAS* 371:55-9
- Dayal P, Ferrara A, Gallerani S. 2008. *MNRAS* 389:1683-96
- Diemand J, Moore B, Stadel J. 2005. *Nature* 433:389-91
- DiMatteo T, Springel V, Hernquist L. 2005. *Nature* 433:604-7
- Dijkstra M, Haiman Z, Rees MJ, Weinberg DH. 2004. *Ap. J.* 601:666-75
- Dijkstra M, Haiman Z, Mesinger A, Wyithe JSB. 2008. *MNRAS* 391:1961-72
- Dijkstra M, Wyithe JSB. 2010. *MNRAS* 408:352-61
- Dijkstra M, Wyithe JSB, Haiman Z. 2007. *MNRAS* 379:253-9
- Eggen OJ, Lynden-Bell D, Sandage AR. 1962. *Ap. J.* 136:748-66
- Eisenstein DJ, Loeb A. 1995. *Ap. J.* 443:11-17
- Eyles LP, Bunker AJ, Ellis RS, Lacy M, Stanway ER, et al. 2007. *MNRAS* 374:910-30
- Fan X, Carilli CL, Keating B. 2006. *Annu. Rev. Astron. Astrophys.* 44:415-62
- Ferrarese L, Ford H. 2005. *Space Sci. Rev.* 116:523-624
- Ferrarese L, Merritt D. 2000. *Ap. J. Lett.* 539:L9-12
- Fernandez ER, Komatsu E, Iliev IT, Shapiro PR. 2010. *Ap. J.* 710:1089-1110
- Finkelstein SL, Papovich C, Giavalisco M, Reddy NA, Ferguson HC, et al. 2010.

- Ap. J.* 719:1250-73
- Frebel A. 2010. *Astron. Nachr.* 331:474-88
- Frebel A, Bromm V. 2011. *Ap. J.* Submitted (arXiv:1010.1261)
- Frebel A, Kirby EN, Simon JD. 2010. *Nature* 464:72-5
- Freeman K, Bland-Hawthorn J. 2002. *Annu. Rev. Astron. Astrophys.* 40:487-537
- Freese K, Ilie C, Spolyar D, Valluri M, Bodenheimer P. 2010. *Ap. J.* 716:1397-1407
- Furlanetto S, Oh SP, Briggs F. 2006. *Phys. Rep.* 433:181-301
- Gao L, Yoshida N, Abel T, Frenk CS, Jenkins A, Springel V. 2007. *MNRAS* 378:449-68
- Gardner JP, Mather JC, Clampin M, Doyon R, Greenhouse MA, et al. 2006. *Space Sci. Rev.* 123:485-606
- Gebhardt K, Bender R, Bower G, Dressler A, Faber SM, et al. 2000. *Ap. J. Lett.* 539:L13-16
- Geisler D, Smith VV, Wallerstein G, Gonzalez G, Charbonnel C. 2005. *Ap. J.* 129:1428-1442
- Glover SCO. 2005. *Space Sci. Rev.* 117:445-508
- Gnedin NY, Kravtsov AV, Chen HW. 2008. *Ap. J.* 672:765-72
- Gonzalez V, Labbe I, Bouwens RJ, Illingworth G, Franx M, et al. 2010. *Ap. J.* 713:115-30
- Greif TH, Bromm V. 2006. *MNRAS* 373:128-38
- Greif TH, Glover SCO, Bromm V, Klessen RS. 2010. *Ap. J.* 716:510-20
- Greif TH, Johnson JL, Bromm V, Klessen RS. 2007. *Ap. J.* 670:1-14
- Greif TH, Johnson JL, Klessen RS, Bromm V. 2008. *MNRAS* 387:1021-36
- Haiman Z. 2009. In *Astrophysics in the Next Decade*, ed. HA Thronson et al., pp. 385-417. Springer: Dordrecht.

- Haiman Z, Bryan GL. 2006. *Ap. J.* 650:7-11
- Haiman Z, Loeb A. 1997. *Ap. J.* 483:21-37
- Haiman Z, Loeb A. 1998. *Ap. J.* 503:505-17
- Haiman Z, Loeb A. 2001. *Ap. J.* 552:459-63
- Haiman Z, Thoul AA, Loeb A. 1996. *Ap. J.* 464:523-38
- Harrington JP. 1973. *MNRAS* 162:43-52
- Hauser MG, Dwek E. 2001. *Annu. Rev. Astron. Astrophys.* 39:249-307
- Holder GP, Haiman Z, Kaplinghat M, Knox L. 2003. *Ap. J.* 595:13-18
- Hu EM, Cowie LL, Capak P, McMahon RG, Hayashino T, Komiyama Y. 2004. *Astron. J.* 127:563-575
- Hu EM, Cowie LL, Barger AJ, Capak P, Kakazu Y, Trouille L. 2010. *Ap. J.* 725:394-423
- Iliev IT, Shapiro PR, McDonald P, Mellema G, Pen U-L. 2008. *MNRAS* 391:63-83
- Inoue AK, Iwata I, Deharveng JM. 2006. *MNRAS* 371:L1-5
- Iocco F, Bressan A, Ripamonti E, Schneider R, Ferrara A, Marigo P. 2008. *MNRAS* 390:1655-69
- Iwata I, Inoue AK, Matsuda Y, Furusawa H, Hayashino T, et al. 2009. *Ap. J.* 692:1287-93
- Iye M, Ota K, Kashikawa N, Furusawa H, Hashimoto T, et al. 2006. *Nature* 443:186-88
- Jappsen AK, Glover SCO, Klessen RS, Mac Low MM. 2007. *Ap. J.* 660:1332-43
- Jasche J, Ciardi B, Ensslin TA. 2007. *MNRAS* 380:417-29
- Jimenez R, Haiman Z. 2006. *Nature* 440:501-4
- Johnson JL. 2010. *MNRAS* 404:1425-36
- Johnson JL, Bromm V. 2006. *MNRAS* 366:247-56

- Johnson JL, Bromm V. 2007. *MNRAS* 374:1557-68
- Johnson JL, Greif TH, Bromm V. 2007. *Ap. J.* 665:85-95
- Johnson JL, Greif TH, Bromm V. 2008. *MNRAS* 388:26-38
- Johnson JL, Greif TH, Bromm V, Klessen RS, Ippolito J. 2009. *MNRAS* 399:37-47
- Johnson JL, Khochfar S, Greif TH, Durier F. 2011. *MNRAS* 410:919-33
- Karlsson T, Johnson JL, Bromm V. 2008. *Ap. J.* 679:6-16
- Kashikawa N, Shimasaku K, Malkan MA, Doi M, Matsuda Y, et al. 2006. *Ap. J.* 648:7-22
- Kashlinsky A. 2005. *Phys. Rep.* 409:361-438
- Kashlinsky A, Arendt RG, Mather J, Moseley SH. 2005. *Nature* 438:45-50
- Kirby EN, Simon JD, Geha M, Guhathakurta P, Frebel A. 2008. *Ap. J. Lett.* 685:L43-46
- Kitayama T, Yoshida N. 2005. *Ap. J.* 630:675-88
- Kitayama T, Yoshida N, Susa H, Umemura M. 2004. *Ap. J.* 613:631-45
- Komatsu E, Dunkley J, Nolta MR, Bennett CL, Gold B, et al. 2009. *Ap. J. Suppl.* 180:330-76
- Kormendy J, Richstone DO. 1995. *Annu. Rev. Astron. Astrophys.* 33:581-624
- Kramer RH, Haiman Z, Madau P. 2011. *MNRAS* Submitted (arXiv:1007.3581)
- Kravtsov AV, Gnedin OY. 2005. *Ap. J.* 623:650-65
- Kuhlen M, Madau P. 2005. *MNRAS* 363:1069-82
- Labbe I, Gonzalez V, Bouwens RJ, Illingworth GD, Franx M, et al. 2010. *Ap. J. Lett.* 716:L103-108
- Lacey CG, Baugh CM, Frenk CS, Benson A. 2011. *MNRAS* In press (arXiv1004.3545)

- Larson RB. 1998. *MNRAS* 301:569-81
- Latif MA, Zaroubi S, Spaans M. 2011. *MNRAS* 411:1659-70
- Lehnert MD, Nesvadba NPH, Cuby JG, Swinbank AM, Morris S, et al. 2010. *Nature* 467:940-42
- Li Y, Hernquist L, Robertson B, Cox TJ, Hopkins PF, et al. 2007. *Ap. J.* 665:187-208
- Lidz A, Zahn O, Furlanetto S, McQuinn M, Hernquist L, Zaldarriaga M. 2009. *Ap. J.* 690:252-66
- Lodato G, Natarajan P. 2006. *MNRAS* 371:1813-23
- Lodato G, Natarajan P. 2007. *MNRAS* 377:L64-8
- Loeb A. 2010. *How Did the First Stars and Galaxies Form?* Princeton, NJ: Princeton Univ. Press
- Loeb A, Rasio FA. 1994. *Ap. J.* 432:52-61
- Loeb A, Rybicki G. 1999. *Ap. J.* 524:527-35
- Maccio AV, Kang X, Fontanot F, Somerville RS, Koposov S, Monaco P. 2010. *MNRAS* 402:1995-2008
- Mashchenko S, Wadsley J, Couchman HMP. 2008. *Science* 319:174-176
- Machida MN, Tomisaka K, Nakamura F, Fujimoto MY. 2005. *Ap. J.* 622:39-57
- Madau P, Ferrara A, Rees MJ. 2001. *Ap. J.* 555:92-105
- Madau P, Haardt F, Rees MJ. 1999. *Ap. J.* 514:648-59
- Madau P, Rees MJ. 2001. *Ap. J. Lett.* 551:L27-30
- Maio U, Dolag K, Ciardi B, Tornatore L. 2007. *MNRAS* 379:963-73
- Maio U, Ciardi B, Dolag K, Tornatore L, Khochfar S. 2010. *MNRAS* 407:1003-15
- Maio U, Khochfar S, Johnson JL, Ciardi B. 2011. *MNRAS* In press (arXiv:1011.3999)

- Malhotra S, Rhoads JE. 2004. *Ap. J. Lett.* 617:L5-8
- Martin NF, de Jong JTA, Rix HW. 2008. *Ap. J.* 684:1075-92
- Mayer L, Kazantzidis S, Escala A, Callegari S. 2010. *Nature* 466:1082-4
- McKee CF, Ostriker EC. 2007. *Annu. Rev. Astron. Astrophys.* 45:565-687
- McKee CF, Tan JC. 2008. *Ap. J.* 681:771-97
- McQuinn M, Hernquist L, Zaldarriaga M, Dutta S. 2007. *MNRAS* 381:75-96
- Meiksin AA. 2009. *Rev. Mod. Phys.* 81:1405-69
- Mesinger A, Dijkstra M. 2008. *MNRAS* 390:107a-801
- Mesinger A, Bryan GL, Haiman Z. 2009. *MNRAS* 399:1650-6
- Milosavljevic M, Bromm V, Couch SM, Oh SP. 2009a. *Ap. J.* 698:766-80
- Milosavljevic M, Couch SM, Bromm V. 2009b. *Ap. J. Lett.* 696:L146-49
- Miralda-Escudé J. 2003. *Science* 300:1904-9
- Mo H, van den Bosch F, White SDM. 2010. *Galaxy Formation and Evolution*.
Cambridge: Cambridge Univ. Press
- Mobasher B et al. 2005. *Ap. J.* 635:832-44.
- Morales MF, Wyithe JSB. 2010. *Annu. Rev. Astron. Astrophys.* 48:127-71
- Moore B, Diemand J, Madau P, Zemp M, Stadel, J. 2006. *MNRAS* 368:563-570
- Mori M, Ferrara A, Madau P. 2002. *Ap. J.* 571:40-55
- Mukherjee P, Liddle AR. 2008. *MNRAS* 389:231-36
- Nagakura T, Omukai K. 2005. *MNRAS* 364:1378-86
- Nagao T, Motohara K, Maiolino R, Marconi A, Taniguchi Y, et al. 2005. *Ap. J. Lett.* 631:L5-8
- Naoz S, Noter S, Barkana R. 2006. *MNRAS* 373:L98-102
- Neufeld D. 1990 *Ap. J.* 350:216-41
- Norris JE, Gilmore G, Wyse RFG, Yong D, Frebel A. 2010a. *Ap. J. Lett.*

722:L104-9

Norris JE, Wyse RFG, Gilmore G, Yong D, Frebel A, et al. 2010b. *Ap. J.*

723:1632-50

Obreschkow D, Heywood I, Klockner HR, Rawlings S. 2009. *Ap. J.* 702:1321-35

Oh SP. 1999. *Ap. J.* 527:16-30

Oh SP. 2001. *Ap. J.* 553:499-512

Oh SP, Haiman Z. 2002. *Ap. J.* 569:558-72

Oke JB. 1974. *Ap. J. Suppl.* 27:21-35

Oke JB, Gunn J. 1983. *Ap. J.* 266:713-7

Omukai K, Hosokawa T, Yoshida N. 2010. *Ap. J.* 722:1793-1815

Omukai K, Palla F. 2003. *Ap. J.* 589:677-87

Omukai K, Schneider R, Haiman Z. 2008. *Ap. J.* 686:801-14

Omukai K, Tsuribe T, Schneider R, Ferrara A. 2005. *Ap. J.* 626:627-43

O'Shea BW, Norman ML. 2008. *Ap. J.* 673:14-33

Ouchi M, Mobasher B., Shimasaku K, Ferguson HC, Fall SM, et al. 2009. *Ap. J.*

706:1136-51

Ouchi M, Shimasaku K, Furusawa H, Saito T, Yoshida M, et al. 2010. *Ap. J.*

723:869-894

Panagia N. 2005. In *The Initial Mass Function 50 Years Later*, ed. E Corbelli et

al., pp.479-86. Dordrecht: Springer

Partridge RB, Peebles PJE. 1967. *Ap. J.* 147:868-86

Pawlik A, Milosavljevic M, Bromm V. 2011. *Ap. J.* In press (arXiv:1011.0438)

Pelupessy, F. Di Matteo, T. Ciardi, B. 2007. *Ap. J.* 665:107-19

Press WH, Schechter P. 1974. *Ap. J.* 187:425-38

Raicevic M, Theuns T, Lacey C. 2011 *MNRAS* 410:775-87

- Raiter A, Schaerer D, Fosbury RAE. 2010. *Astron. Astrophys* 523:64
- Razoumov AO, Sommer-Larsen J. 2010. *Ap. J.* 710:1239-46
- Rees MJ. 1984. *Annu. Rev. Astron. Astrophys.* 22:471-506
- Rees MJ. 1993. *Quart. J. Roy. Astron. Soc.* 34:279-89
- Regan JA, Haehnelt MG. 2009a. *MNRAS* 393:858-71
- Regan JA, Haehnelt MG. 2009b. *MNRAS* 396:343-53
- Ricotti M. 2010. *Advances in Astronomy* (DOI:10.1155/2010/271592)
- Ricotti M, Gnedin NY, Shull JM. 2002. *Ap. J.* 575:33-48
- Ricotti M, Gnedin NY, Shull JM. 2002. *Ap. J.* 575:49-55
- Ricotti M, Gnedin NY, Shull JM. 2008. *Ap. J.* 685:21-39
- Ricotti M, Ostriker JP. 2004. *MNRAS* 352:547-62
- Ripamonti E, Mapelli M, Ferrara A. 2007. *MNRAS* 375:1399-1408
- Robertson BE, Ellis RS, Dunlop JS, McLure RJ, Stark DP. 2010. *Nature* 468:49-55
- Ryan-Weber EV, Pettini M, Madau P, Zych BJ. 2009. *MNRAS* 395:1476-90
- Safrank-Shrader C, Bromm V, Milosavljevic M. 2010. *Ap. J.* 723:1568-82
- Salpeter EE. 1955. *Ap. J.* 121:161-67
- Salvadori S, Ferrara A. 2009. *MNRAS* 395:L6-10
- Salvaterra R, Ferrara A. 2003. *MNRAS* 339:973-82
- Salvaterra R, Ferrara A, Dayal P. 2011. *MNRAS* In press (arXiv:1003.3873)
- Santoro F & Shull JM. 2006. *Ap. J.* 643:26-37
- Santos MR. 2004 *MNRAS* 349:1137-52
- Santos MR, Bromm V, Kamionkowski M. 2002. *MNRAS* 336:1082-92
- Scannapieco E, Madau P, Woosley SE, Heger A, Ferrara A. 2005. *Ap. J.* 633:1031-

- Schaerer D. 2002. *Astron. Astrophys.*, 382:28-42
- Schaerer D. 2003. *Astron. Astrophys.*, 397:527-38
- Schleicher DRG, Banerjee R, Sur S, Arshakian TG, Klessen RS, Beck R, Spaans M. 2010. *Astron. Astrophys.* 522:115
- Schneider R, Ferrara A, Natarajan P, Omukai K. 2002. *Ap. J.* 571:30-39
- Schneider R, Omukai K, Inoue AK, Ferrara A. 2006. *MNRAS* 402:429-35
- Schneider R, Omukai K. 2010. *MNRAS* 402:429-35
- Shang C, Bryan GL, Haiman Z. 2010. *MNRAS* 385:1249-62
- Shapley AE, Steidel CC, Pettini M, Adelberger KL, Erb DK. 2006. *Ap. J.* 651:688-703
- Siana B, Teplitz HI, Colbert J, Ferguson HC, Dickinson M, et al. 2007. *Ap. J.* 668:62-73
- Simcoe RA. 2006. *Ap. J.* 653:977-87
- Simon JD, Geha M, Minor QE, Martinez GD, Kirby EN, et al. 2011. *Ap. J.* Submitted (arXiv:1007.4198)
- Smith BD, Sigurdsson S. 2007. *Ap. J. Lett.* 661:L5-8
- Smith BD, Sigurdsson S, Abel T. 2008. *MNRAS* 385:1443-1454
- Sokasian A, Yoshida N, Abel T, Springel V, Hernquist L. 2004. *MNRAS* 350:47-65
- Songaila A. 2001. *Ap. J.* 561:L153-56
- Spaans M, Silk J. 2006. *Ap. J.* 652:902-6
- Spolyar D, Freese K, Gondolo P. 2008. *Phys. Rev. Lett.* 100:051101
- Springel V, White SDM, Jenkins A., Frenk CS, Yoshida N, et al. 2005. *Nature* 435:629-636
- Stacy A, Bromm V. 2007. *MNRAS* 382:229-38
- Stark DP, Bunker AJ, Ellis RS, Eyles LP, Lacey MA. 2007. *Ap. J.* 659:84-97

Stiavelli M. 2009. *From First Light to Reionization: The End of the Dark Ages.*

Weinheim: Wiley-VCH

Stiavelli M, Fall SM, Panagia N. 2004. *Ap. J.* 600:508-19

Susa H. 2008. *Ap. J.* 648:226-35

Tanaka T, Haiman Z. 2009. *Ap. J.* 696:1798-822

Taniguchi Y, Shioya Y, Trump JR. 2010. *Ap. J.* 724:1480-490

Tegmark M, Silk J, Rees MJ, Blanchard A, Abel T, Palla F. 1997. *Ap. J.* 474:1-12

Thompson RI, Eisenstein D, Fan X, Rieke M, Kennicutt RC. 2007. *Ap. J.* 666:658-

62

Tolstoy E, Hill V, Tosi M. 2009. *Annu. Rev. Astron. Astrophys.* 47:371-425

Tolstoy E et al. 2004. *Ap. J. Lett.* 617:119-22

Tornatore L, Ferrara A, Schneider R. 2007. *MNRAS* 382:945-50

Trenti M, Stiavelli M. 2006. *Ap. J.* 651:704-12

Trenti M, Stiavelli M. 2008. *Ap. J.* 676:767-80

Trenti M, Stiavelli M. 2009. *Ap. J.* 694:879-92

Tumlinson J. 2010. *Ap. J.* 708:1398-418

Tumlinson J, Shull JM. 2000. *Ap. J. Lett.* 528:L65-68

Umeda H, Yoshida N, Nomoto K, Tsuruta S, Sasaki M, Ohkubo T. 2009. *JCAP*

08:24

Vasiliev EO, Shchekinov YA. 2006. *Astron. Rep.* 50:778-84

Volonteri M, Rees MJ. 2006. *Ap. J.* 650:669-78

Volonteri M, Natarajan P. 2009. *MNRAS* 400:1911-18

Wada K, Venkatesan A. 2003. *Ap. J.* 591:38-42

Walter F, Carilli C. 2007. In *Frontiers in Astronomy*, ed. Bridle AH et al. ASP

Conference series Vol. 395.

- Whalen D, Abel T, Norman ML. 2004. *Ap. J.* 610:14-20
- Whalen D, Bromm V, Yoshida N, eds. 2010. *The First Stars and Galaxies: Challenges for the Next Decade*. AIP Conf. Proc. 1294. Melville, New York: AIP
- Whalen D, van Veelen B, O'Shea BW, Norman ML. 2008. *Ap. J.* 682:49-67
- Wiklind T et al. 2008. *Ap. J.* 676:781-806.
- Wise JH, Abel T. 2007. *Ap. J.* 665:899-910
- Wise JH, Abel T. 2008. *Ap. J.* 685:45-56
- Wise JH, Cen R. 2009. *Ap. J.* 693:984-99
- Wise JH, Turk MJ, Abel T. 2008 *Ap. J.* 682:745-57
- Wise JH, Turk MJ, Norman ML, Abel T. 2011. *Ap. J. Lett.* Submitted
- Wolcott-Green J, Haiman Z. 2010. *MNRAS* In press (arXiv:1009.1087)
- Yajima H, Umemura M, Mori M, Nakamoto T. 2009. *MNRAS* 398:715-21
- Yajima H, Choi JH, Nagamine K. 2011. *MNRAS* In press (arXiv:1002.3346)
- Yoshida N, Abel T, Hernquist L, Sugiyama N. 2003. *Ap. J.* 592:645-63
- Yoshida N, Bromm V, Hernquist L. 2004. *Ap. J.* 605:579-90
- Yoshida N, Oh SP, Kitayama T, Hernquist L. 2007a. *Ap. J.* 663:687-707
- Yoshida N, Omukai K, Hernquist L. 2007b. *Ap. J. Lett.* 667:L117-120
- Yoshida N, Omukai K, Hernquist L. 2008. *Science* 321:669-71
- Yu Q, Tremaine S. 2002. *MNRAS* 335:965-76
- Zentner, A. 2007. *Int. J. Mod. Phys. D* 16:753-815
- Zheng Z, Cen R, Trac H, Miralda-Escud J. 2010. *Ap. J.* 716:574-98
- Zinnecker H, Yorke HW. 2007. *Annu. Rev. Astron. Astrophys.* 45:481-563

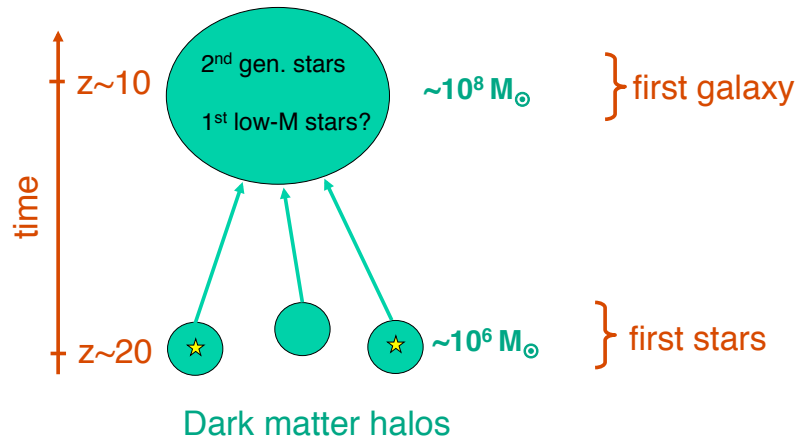


Figure 1: Assembly of the first galaxy. We here illustrate the scenario where the first galaxies reside in atomic cooling halos. These comprise total masses of $\sim 10^8 M_\odot$ and typically collapse at $z \sim 10$. Note that within the scenario illustrated in this figure, minihalos are not considered galaxies, because of the strong negative feedback from the Pop III stars that form inside of them. This feedback will effectively destroy the minihalos such that neither gas nor low-mass stars will remain in them. Their assembly is affected by the feedback from the first (Pop III) stars that had formed earlier in the minihalo progenitor systems. Within this model, atomic cooling halos hosted the second generation of stars, including the first low-mass (Pop II) stars that could have survived to the present day.

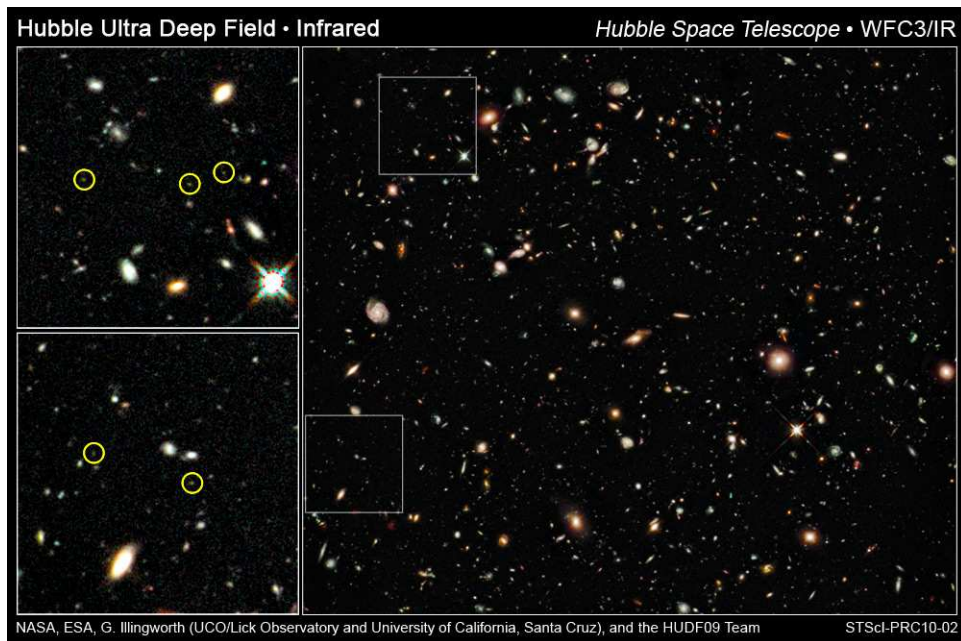


Figure 2: Early galaxies in HST's deepest view of the Universe. The image was taken with the newly installed WFC3/IR camera, with the positions of newly discovered galaxies at $z \simeq 7 - 8$ indicated by the circles in the zooms on the left-hand side. Figure courtesy of NASA.

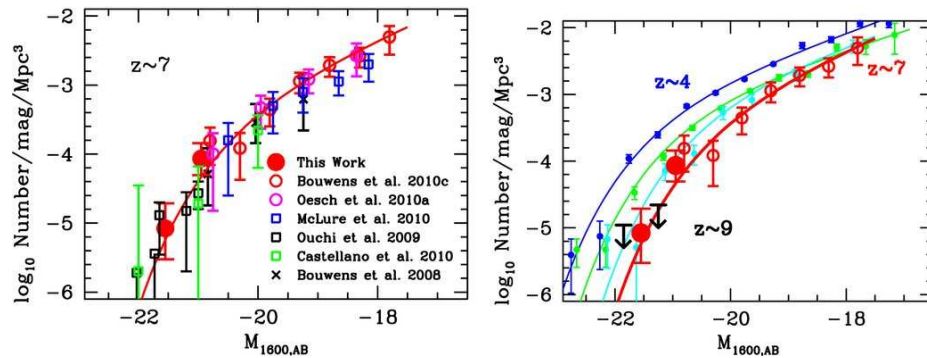


Figure 3: UV luminosity function at $z \sim 7$. Shown is the number density of sources per unit magnitude vs. the absolute (soft) UV AB magnitude. *Left panel:* LF at $z \sim 7$, as derived from HST NICMOS and ground-based observations (large solid red circles), together with other determinations, as labelled in the figure. Overplotted is the best-fit Schechter function (solid red line). *Right panel:* A comparison of the UV LF at $z \sim 7$ (solid red circles), with those at $z \sim 6$ (cyan), $z \sim 5$ (green), and $z \sim 4$ (blue). Evidently the LF evolves over the redshift interval considered here. Adopted from Bouwens et al. (2010a).

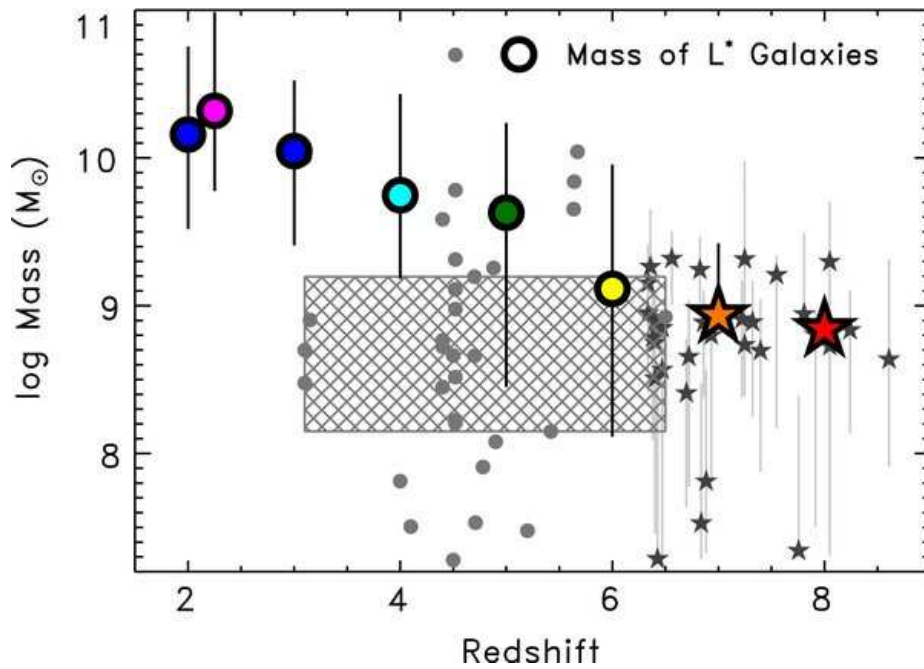


Figure 4: Stellar mass of high-redshift galaxies. The colored symbols represent data for LBGs with characteristic luminosity (L^*). It is evident that stellar masses in typical LBGs decreases with redshift. The small grey circles denote LAEs for comparison, and the grey hatched region shows the interquartile range. The highest redshift LBGs seem to be more similar to the LAEs than to LBGs at lower redshift. Adopted from Finkelstein et al. (2010), where all references for the data shown here can be found.

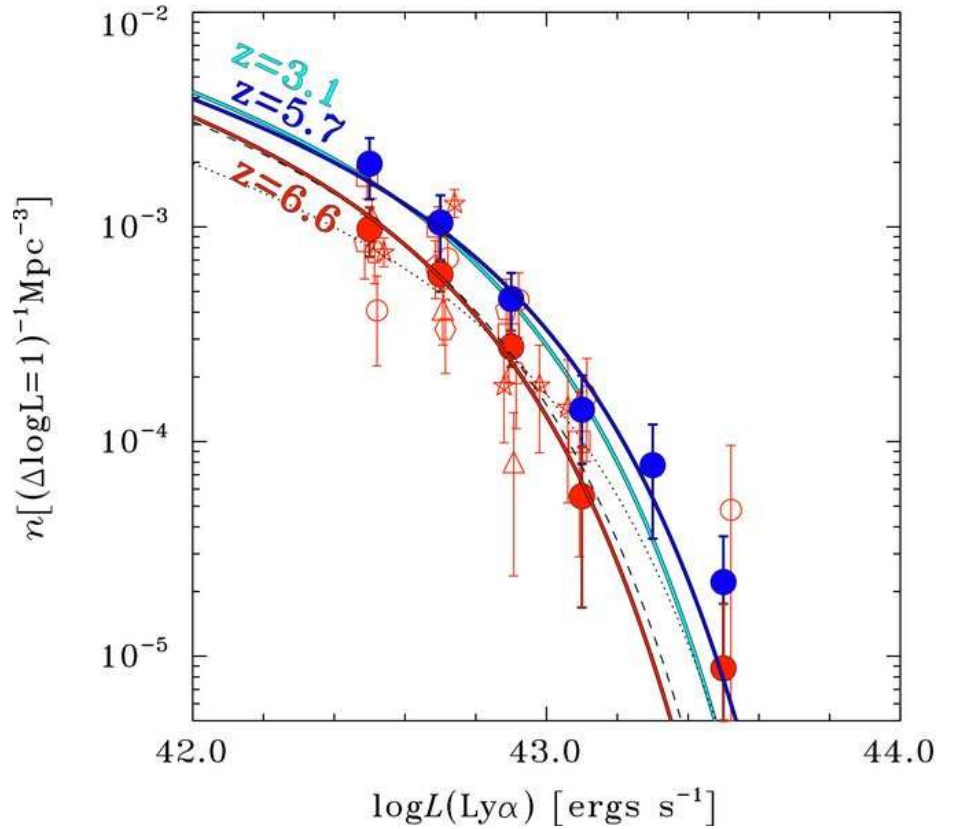


Figure 5: Evolution of Lyman- α luminosity function. Shown is the number density of LAEs vs. Lyman- α luminosity for three different redshifts, as labelled in the plot. The $z = 6.6$ data was derived from the 1 deg^2 wide Subaru/XMM-Newton Deep Survey (SXDS) field, to be compared with previous measurements of the LF at lower redshifts. Solid lines give various fits to the Schechter function. It is evident that there is very little evolution from $z = 3.1$ (*cyan solid line*) to $z = 5.7$ (*blue filled circles and solid line*), but significant evolution towards $z = 6.6$ (*red filled circles and solid line*). The open symbols show the less precise results from smaller, 0.2 deg^2 , fields, which cannot reliably establish whether evolution is present or not. This demonstrates the need for wide-field surveys to measure high- z LFs with the required precision. Adopted from Ouchi et al. (2010).

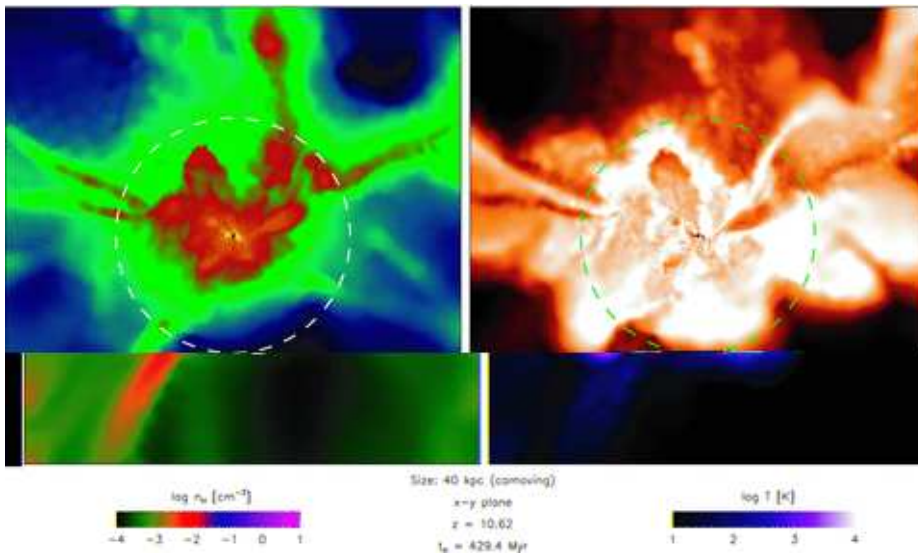


Figure 6: Turbulent collapse into the first galaxy. Shown is the hydrogen number density (*left-hand panel*) and temperature (*right-hand panel*) in the inner 4 kpc (physical), surrounding the BH at the center of the galaxy, indicated by the filled black circle. The dashed lines denote the virial radius at a distance of 1 kpc. Hot accretion dominates where gas is accreted directly from the IGM and shock-heated to 10^4 K. In contrast, cold accretion becomes important as soon as gas cools in filaments and flows towards the center of the galaxy. These cold streams drive a prodigious amount of turbulence and create transitory density perturbations that could in principle become Jeans-unstable. Adopted from Greif et al. (2010).

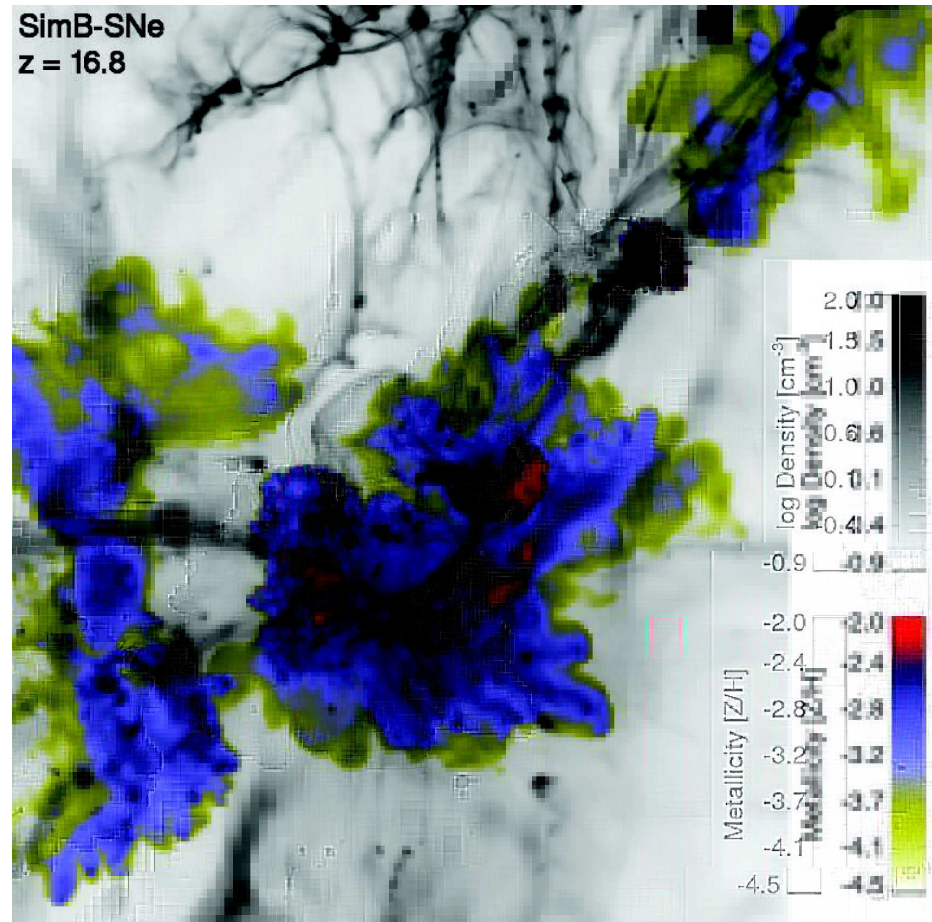


Figure 7: Metal enrichment in the first galaxy. Shown is the aftermath of tens of pair-instability supernovae (PISNe) which exploded inside the progenitor mini-halos. The situation here corresponds to $z \simeq 17$. The projection of metallicity is shown in color, and that of gas density in shades of grey, with values indicated by the insets. The box has a proper size of 8.6 kpc. Adopted from Wise & Abel (2008).

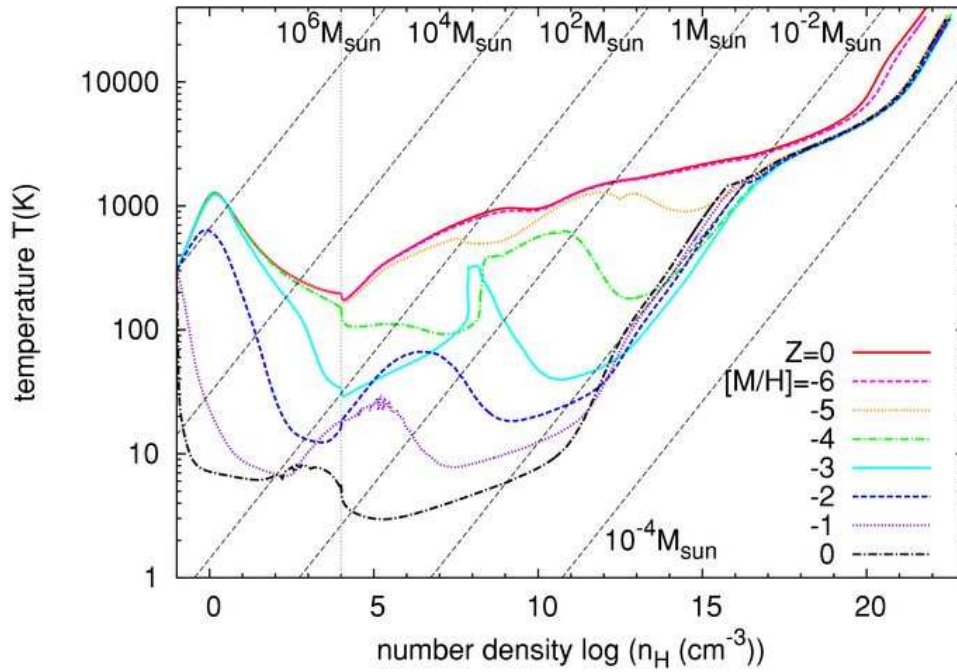


Figure 8: Thermal evolution of pre-stellar gas with various metallicities. The constant Jeans masses are indicated by the dashed lines. Characteristic temperature dips are caused by cooling due to atomic line cooling at low densities, molecular cooling at intermediate densities, and dust thermal emission at high densities. Adopted from Omukai, Hosokawa & Yoshida (2010).

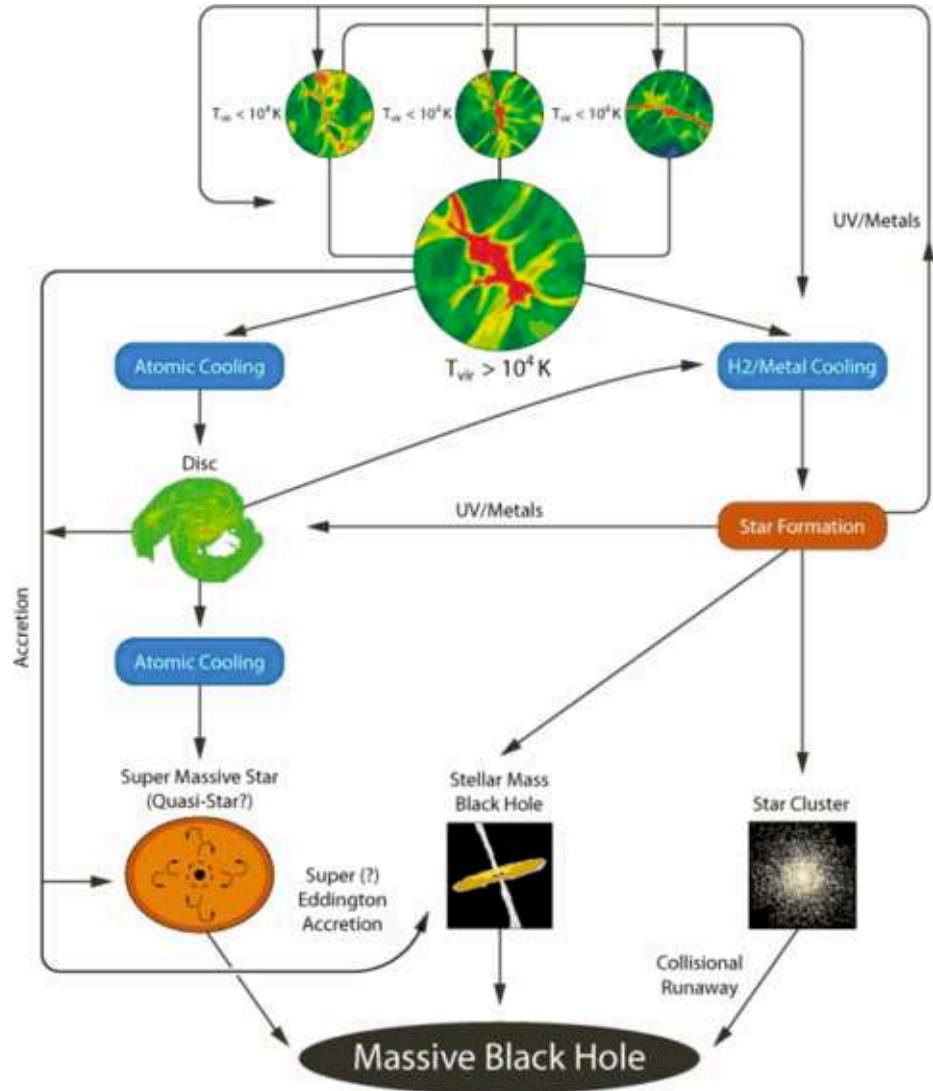


Figure 9: Pathways towards the first supermassive black holes. Here, possible SMBH formation channels in high-redshift atomic cooling halos are shown. The main bifurcation arises from whether the gas inside the first galaxy can cool below $\sim 10^4 \text{ K}$, via H₂ or metal cooling, or not. If the gas can cool, star formation will ensue. SMBH formation would then have to rely on stellar-dynamical processes of catastrophic runaway collisions. In the opposite case, the path towards a SMBH involves gas-dynamical processes, possibly resulting in the intermediate stage of a supermassive star (or quasi-star). Such a star would rapidly turn into a SMBH. Adopted from Regan & Haehnelt (2009b).

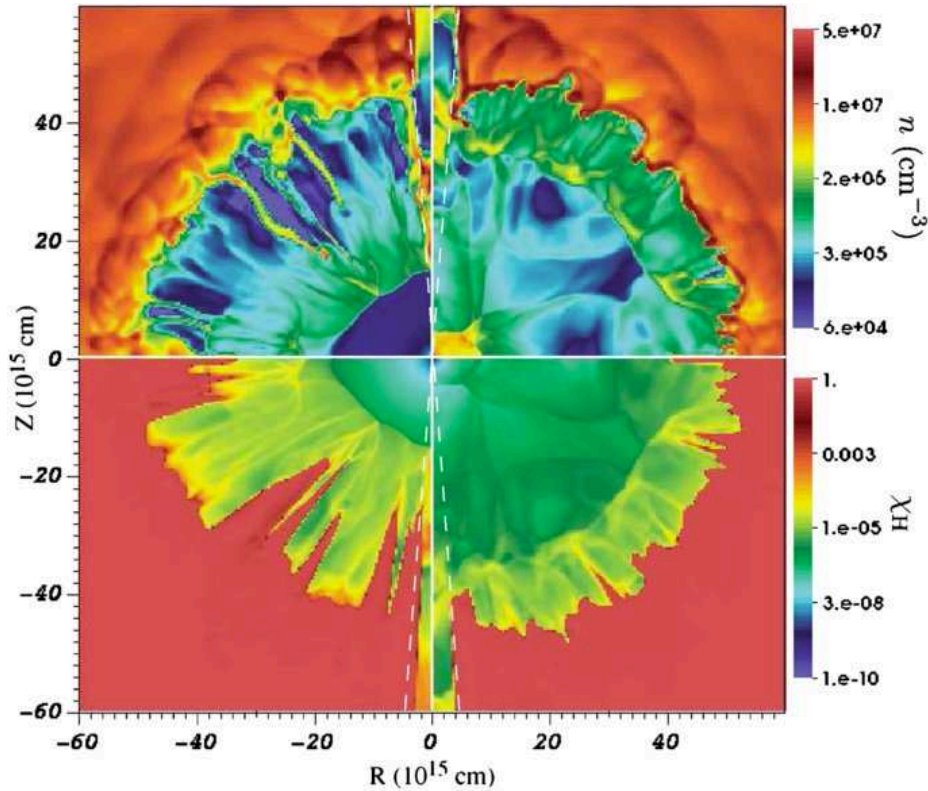


Figure 10: Accretion onto the first black holes. Gas number densities n (*top row*), and neutral fraction χ_{H} (*bottom row*) in the vicinity of the accreting black hole. Shown is the situation during an accretion minimum (*left column*), and during a maximum (*right column*). At maximum, central densities are high, and the H II region grows in response. The structure near the vertical axis (*dashed lines*) is a numerical artifact. The resulting hydrodynamics is complex, exhibiting overlapping in- and outflows that establish an episodic pattern of accretion and radiation-pressure feedback. Adopted from Milosavljevic, Couch & Bromm (2009b).

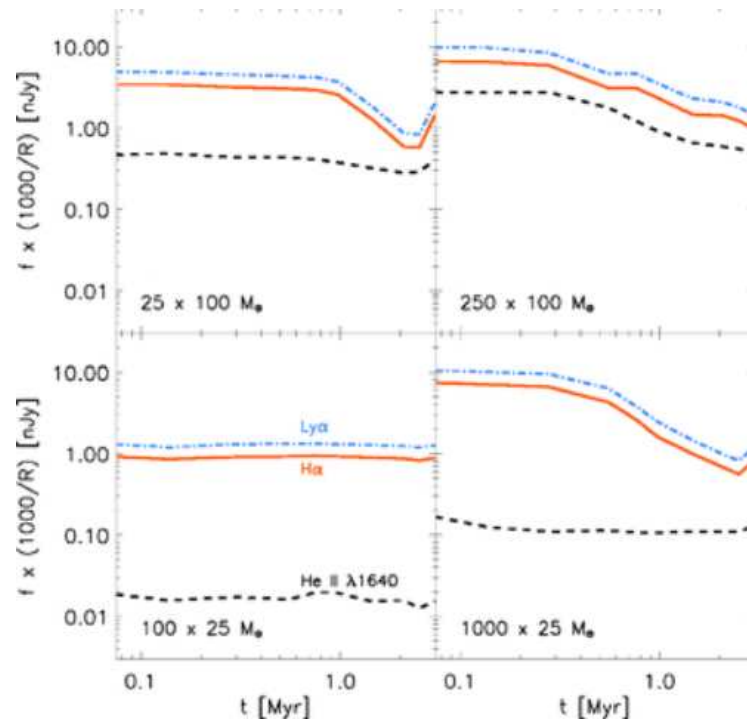


Figure 11: Emission line fluxes in the first galaxies. Shown are predictions for observable recombination line fluxes as a function of time. The source is an atomic cooling halo at $z \simeq 12.5$. The lines are: Ly α (dot-dashed blue), H α (solid red) and He II 1640 Å (dashed black). The fluxes are normalized to a spectral resolution of $R = 1000$. The Ly α flux is an upper limit, due to the possibly severe attenuation by the surrounding, still largely neutral, IGM. Adopted from Johnson et al. (2009).

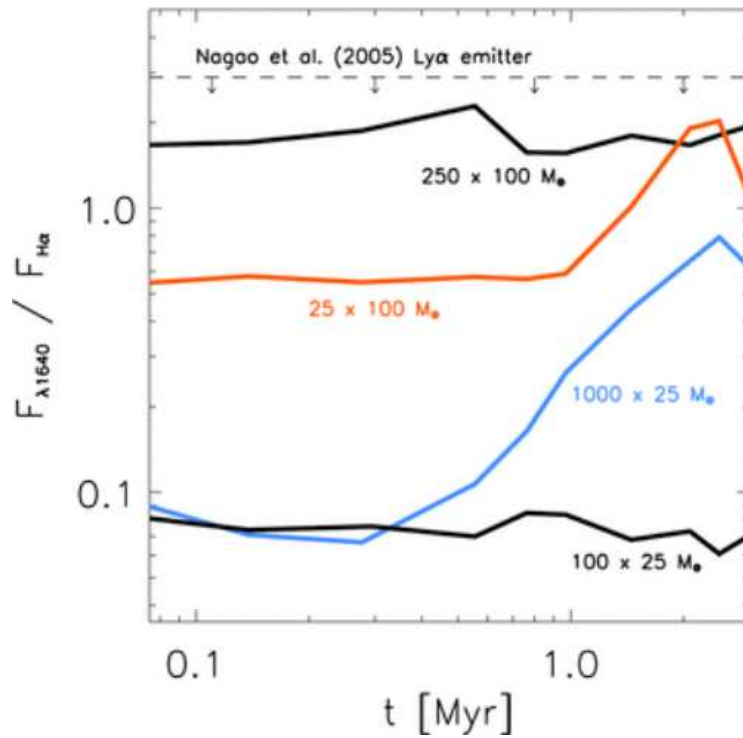


Figure 12: IMF diagnostics in the first galaxies. Shown is the flux ratio in the He II 1640 Å to H α recombination line as a function of time. The calculation assumes a central cluster of Pop III stars, all either with a mass of $25M_{\odot}$ or $100M_{\odot}$ for simplicity. The more massive Pop III stars lead to a ratio that is an order of magnitude larger, thus enabling to diagnose the nature of the stellar population. The dashed horizontal line corresponds to the upper limit for the strong Lyman- α emitter SDF J132440.6+273607 at $z \simeq 6.3$ (Nagao et al. 2005). Evidently, this limit does not yet allow to distinguish between different populations. Adopted from Johnson et al. (2009).

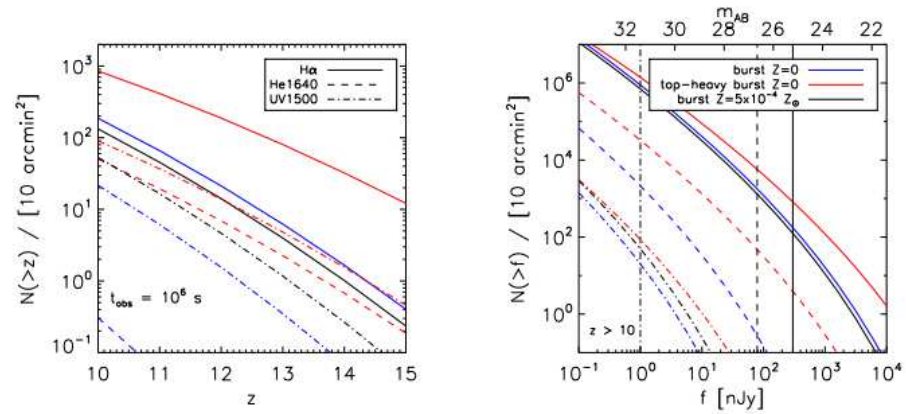


Figure 13: *JWST* number counts of the first galaxies. The calculations assume $t_{\text{exp}} = 10^6$ s and $S/N = 10$. *Left panel*: Number of galaxies $N(> z)$ with redshifts $z > 10$ hosting a starburst observable through the detection of $\text{H}\alpha$ (solid lines), $\text{He II } 1640 \text{ \AA}$ (dashed lines), or the soft UV continuum (dash-dotted lines). Colors denote different choices for stellar metallicity and IMF, as described in the inset of the right-hand panel. *Right panel*: Number of galaxies $N(> f)$ above $z > 10$ with observed fluxes $> f$. The vertical lines show the *JWST* flux limits for $\text{H}\alpha$ (solid), $\text{He II } 1640 \text{ \AA}$ (dashed), and the soft UV continuum (dash-dotted). *JWST* may detect a few tens (for $Z > 0$ and normal IMF) up to a thousand (for Pop III with a top-heavy IMF) starbursts from $z > 10$ in its field-of-view of $\sim 10 \text{ arcmin}^2$. Adopted from Pawlik, Milosavljevic & Bromm (2011).

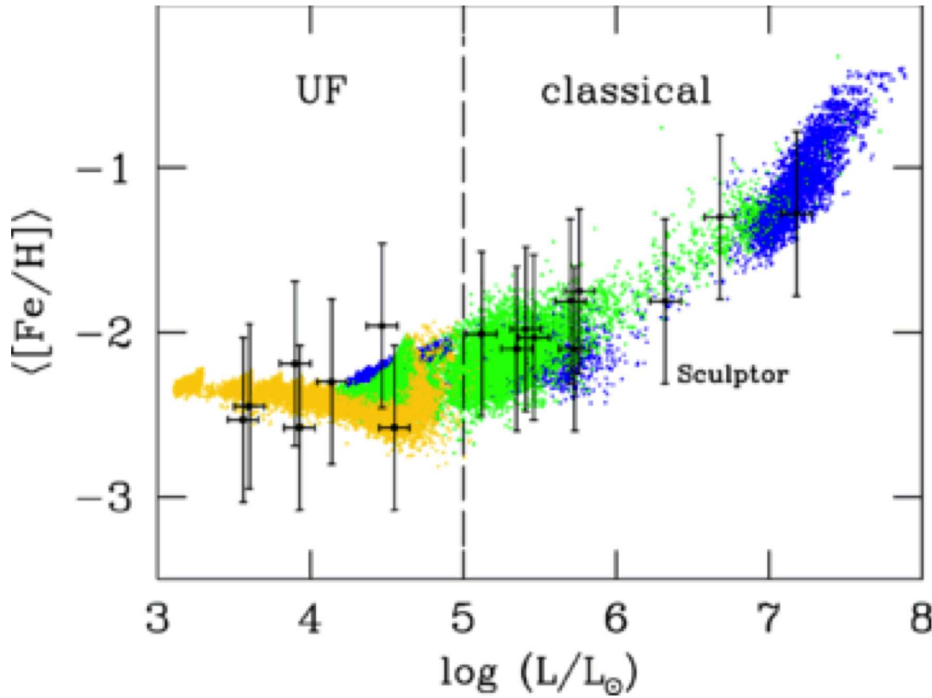


Figure 14: Stellar archaeology with dwarf galaxies. Shown are average Fe abundances vs. total luminosities for dwarf galaxies as predicted by a semi-analytical merger tree model. Different colors indicate the baryon fraction at the time of formation, expressed relative to the cosmic mean: $f_b/\bar{f}_b > 0.5$ (blue dots), $0.1 < f_b/\bar{f}_b < 0.5$ (green), and $f_b/\bar{f}_b < 0.1$ (yellow). The symbols with error bars denote observational data from Kirby et al. (2008). Within this model, the ultra-faint (UF) dwarf galaxies are the fossils of minihalos with (virial) masses close to the limit where atomic cooling would set in ($M \simeq 10^7 - 10^8 M_{\odot}$). The classical dwarf spheroidals, such as the prototypical Sculptor system, would then be descendants of more massive dark matter halos. Adopted from Salvadori & Ferrara (2009).